NASA Technical Memorandum 102889   USAAVSCOM Technical Report 90-A-008

Development and Evaluation of an Inverse Solution Technique for Studying Helicopter Maneuverability and Agility

Matthew S. Whalley

July 1991

US Army
Aviation Systems Command
Moffett Field, CA 94035-1000

NASA
National Aeronautics and
Space Administration

Development and Evaluation of an Inverse Solution Technique for Studying Helicopter Maneuverability and Agility

Matthew S. Whalley, Aeroflightdynamics Directorate, U. S. Army Aviation Systems Command, Ames Research Center, Moffett Field, California

Contents

CONCLUDING REMARKS 35

APPENDIX A – MATH MODEL 37

APPENDIX B – DEFINITION OF MANEUVERABILITY AND AGILITY 43

REFERENCES 49

NOMENCLATURE

A	rotor disk area, ft^2
c_{max}	upper collective limit, in.
c_{min}	lower collective limit, in.
c_{trim}	collective trim position, in.
$K_{overshoot}$	overshoot coefficient, nd
L_p	roll damping coefficient, 1/sec
L_{δ_a}	roll control power, rad/sec^2/in.
$L_{\delta_{a_k}}$	normalizing roll control power coefficient, rad/sec/in.
L_{p_b}	roll damping function intercept, 1/sec
L_{p_m}	roll damping function slope, 1/sec/g
M_q	pitch damping coefficient, 1/sec
M_{δ_e}	pitch control power, rad/sec^2/in.
$M_{\delta_{e_k}}$	normalizing pitch control power coefficient, rad/sec/in.
M_{q_b}	pitch damping function intercept, 1/sec
M_{q_m}	pitch damping function slope, 1/sec/g
N_ϕ	change in yaw moment with roll angle, 1/sec^2/rad
N_p	change in yaw moment with roll rate, 1/sec
N_r	yaw damping coefficient, 1/sec
N_v	change in yaw moment with sideward velocity, ft-rad/sec
N_x	longitudinal acceleration, g
N_y	lateral acceleration, g
N_z	load factor, g
N_{δ_p}	yaw control power, rad/sec^2/in.
$N_{z_{maxc}}$	maximum continuous load factor, g
$N_{z_{maxt}}$	maximum transient load factor, g
$N_{z_{mint}}$	minimum transient load factor, g
$N_{z_{maxc_{hover}}}$	maximum continuous load factor in hover, g
p	roll rate, rad/sec
P_s	specific excess power, ft/min
q	pitch rate, rad/sec
r	yaw rate, rad/sec
R	rotor radius, ft
t	time, sec
T	main rotor thrust, lbf
T_∞	main rotor thrust out of ground effect, lbf
T_g	main rotor thrust in ground effect, lbf
u	body axis longitudinal velocity, ft/sec
v	body axis lateral velocity, ft/sec
V	total airspeed, ft/sec
v_i	main rotor induced velocity, ft/sec
w	body axis vertical velocity, ft/sec
w_{trim}	body axis vertical velocity for level flight, ft/sec
X_u	longitudinal damping, 1/sec
Y_v	lateral damping, 1/sec
z	height above ground, ft

Z_r	reference Z acceleration for trim flight, ft/sec^2
Z_w	vertical damping, 1/sec
Z_{δ_c}	collective control power, ft/sec^2/in.
$Z_{\delta_{c_b}}$	collective control power function intercept, ft/sec^2/in.
$Z_{\delta_{cm}}$	collective control power function slope, ft/sec^2/in.^{2}
$Z_{\delta_{c_{max}}}$	maximum collective control power at a given flight condition, ft/sec^2/in.
$Z_{\delta_{c_{min}}}$	maximum collective control power at a given flight condition, ft/sec^2/in.
Z_{ge}	ground effect portion of Z force equation, ft/sec^2
β	sideslip angle, rad
χ	flight path heading, rad
δ_a	lateral stick input, in.
δ_c	collective stick perturbation from trim, in.
δ_e	longitudinal stick input, in.
δ_p	pedal input, in.
$\delta_{a_{deadzone}}$	lateral stick deadzone, in.
$\delta_{a_{max}}$	maximum lateral stick input, in.
$\delta_{c_{max}}$	maximum positive collective perturbation from trim, in.
$\delta_{c_{min}}$	maximum negative collective perturbation from trim, in.
$\delta_{c_{max_{hover}}}$	maximum positive collective perturbation from trim in hover, in.
$\delta_{e_{deadzone}}$	longitudinal stick deadzone, in.
$\delta_{e_{max}}$	maximum longitudinal stick input, in.
γ	climb angle, rad
ϕ	roll attitude, rad
ϕ_{trim}	trim roll angle, rad
ψ	heading, rad
ρ	density, slug/ft^3
θ	pitch attitude, rad
θ_{trim}	trim pitch attitude, rad

SUMMARY

An inverse solution technique for determining the maximum maneuvering performance of a helicopter using smooth, "pilotlike" control inputs is presented. Also described is a piloted simulation experiment performed on the NASA Ames Advanced Cab and Visual System to investigate the accuracy of the solution resulting from this technique. The maneuverability and agility capability of the helicopter math model was varied by varying the pitch and roll damping, the maximum pitch and roll rate, and the maximum load-factor capability. Three maneuvers were investigated: a 180-degree turn, a longitudinal pop-up, and a lateral jink. The inverse solution technique yielded accurate predictions of pilot-in-the-loop maneuvering performance for two of the three maneuvers.

INTRODUCTION

For the purposes of this study, maneuverability is defined as the maximum achievable time-rate-of-change of the velocity vector at any point in the flight envelope, and agility is defined as the maximum achievable time-rate-of-change of the acceleration vector at any point in the flight envelope. The development of these definitions is discussed in appendix B. The measures of maneuverability used in this study include maximum load-factor capability (both transient and continuous), maximum pitch rate capability, and maximum roll rate capability. The measures of agility used are the bandwidths (damping) of the pitch and roll responses.

Two separate questions must be answered in order to predict the amount of maneuverability and agility (MA) required to perform a specific mission:

1. What minimum level of task performance is required for specific maneuvers?

2. What minimum amount of MA is needed to achieve that performance?

As an example, consider how one would specify MA goals for a 180-degree level turn. One would first need to know how quickly and within what distance the turn would need to be performed in order for it to be effective in a particular mission. One would then determine how much roll-rate and load-factor capability was needed to satisfy the maneuver performance criteria. For a full set of MA design goals for a future rotorcraft to be developed, this process would have to be repeated for a complete set of mission maneuvers. This would be an iterative process as the tradeoffs between the mission definition and final design costs were evaluated. It follows, then, that some fast and direct method of determining the amount of MA needed would be beneficial.

One way of determining the MA required for specific maneuvers is to use an inverse solution approach. Several recent papers have addressed the inverse solution using various techniques (refs. 1-5). The inverse solution technique presented in this report is similar to one used by Thompson (ref. 6) to evaluate the agility of two different helicopters in some simple maneuvers. The technique has been extended here to predict the maximum maneuvering performance of a given configuration, and the extended technique has been implemented as a computer code. This technique solves for control time histories, given a precise flightpath definition, by means of inverse solution of the helicopter equations of motion. By iterating on the task performance requirements, the maximum attainable performance can be determined if the MA capability of a helicopter is known. If the solution if performed in reverse, a more "goal-directed" approach can be taken to the problem of
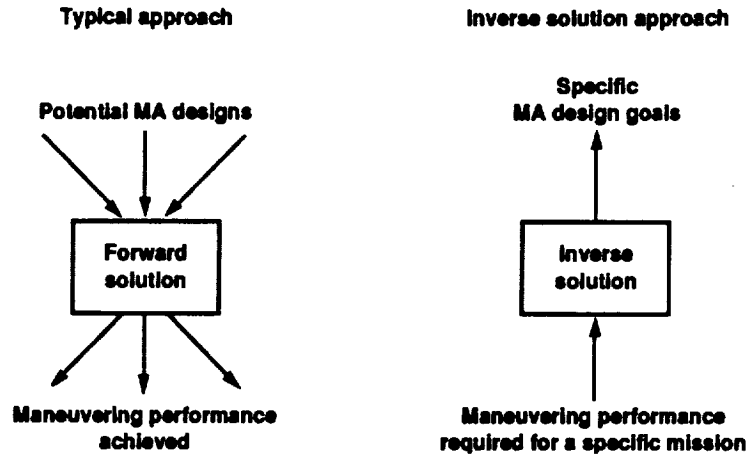
Figure 1. Typical approach versus inverse solution approach to determining maneuverability and agility design goals.

determining how much MA is required. Typically, one would start with a set of potential MA configurations and then solve the equations of motion in a forward manner, thus obtaining a set of maneuvering-performance data (fig. 1). This maneuvering-performance data would then be fitted to the requirements. By using the inverse solution approach, one can start with the specific mission maneuvers of interest, at the performance levels thought necessary, and then carry out the inverse solution analysis, thereby arriving at specific MA requirements. An additional advantage of this method is that the MA tradeoffs for specific performance needs can be carefully examined.

This report (1) presents the inverse solution methodology and some issues associated with it, (2) describes a piloted simulation experiment that was conducted to explore some of these issues, and (3) discusses some results of both the inverse solution analysis and the piloted simulation.

INVERSE SOLUTION ANALYSIS

The method used here for predicting the helicopter control time histories is based on a technique described in reference 6. The technique has been enhanced to calculate the maximum maneuvering performance for a given configuration performing a given maneuver. The process has been implemented as a computer algorithm. This section describes the inverse solution procedure and presents some possible drawbacks associated with its use.

Inverse Solution Procedure

It is easiest to understand the inverse solution by first recalling how a math model is normally used. In a typical math model, the equations of motion are solved to find the dynamic response of the helicopter to a specified control input. By integrating the equations of motion of the helicopter, the flightpath time history can be determined. The inverse solution starts with a specified flightpath, and solves the equations of motion for a unique control time history. Figure 2 shows the overall procedure used during this study for performing the inverse solution.

The 180-degree turn, shown in figure 3, will be used as an example maneuver to illustrate the inverse solution technique. The turn is initiated at 85 knots and terminated at 70 knots, altitude is
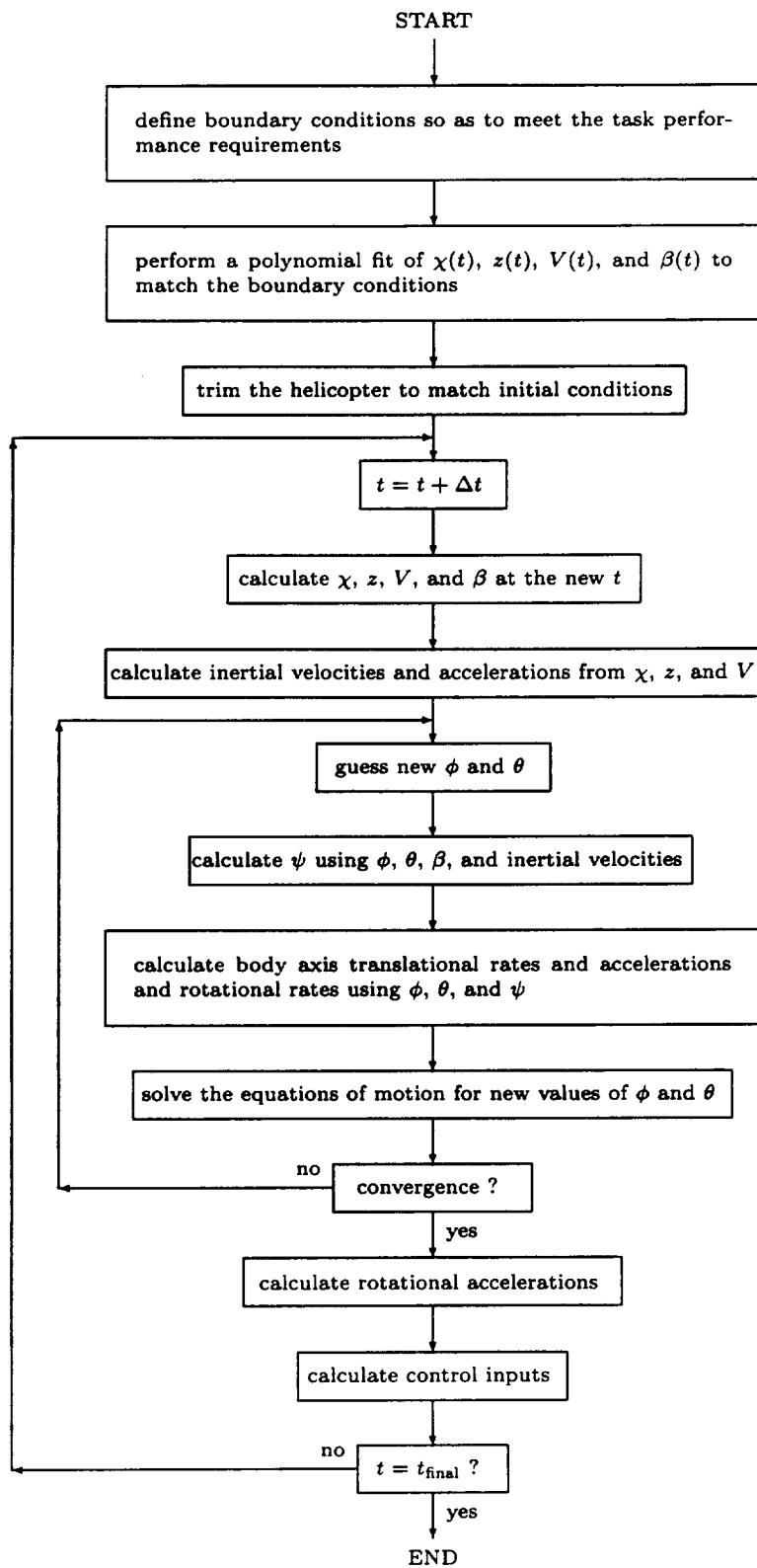
2

START

define boundary conditions so as to meet the task performance requirements

perform a polynomial fit of $\chi(t)$, $z(t)$, $V(t)$, and $\beta(t)$ to match the boundary conditions

trim the helicopter to match initial conditions

$t = t + \Delta t$

calculate χ, z, V, and β at the new t

calculate inertial velocities and accelerations from χ, z, and V

guess new ϕ and θ

calculate ψ using ϕ, θ, β, and inertial velocities

calculate body axis translational rates and accelerations and rotational rates using ϕ, θ, and ψ

solve the equations of motion for new values of ϕ and θ

no

convergence ?

yes

calculate rotational accelerations

calculate control inputs

no

$t = t_{\text{final}}$?

yes

END
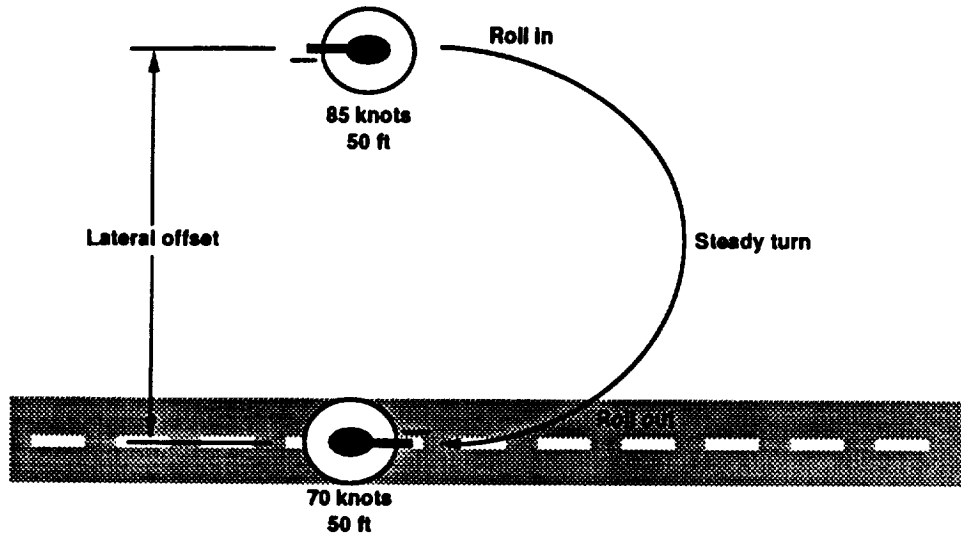
Figure 2. Inverse solution procedure.

3

Figure 3. 180-degree turn.

constant at 50 ft, and the sideslip angle is held to zero throughout the maneuver. For the analysis, the 180-degree turn is broken into three segments: a roll-in portion, a steady-rate-of-turn portion, and a roll-out portion. The roll-in and roll-out are assumed to be of equal time length.

The first step is to define the flightpath boundary conditions in terms of four flightpath state variables. Four variables are required because there are four controls, and a unique mapping from flightpath to controls is desired. The four variables used to define the 180-degree turn are flightpath heading (χ), altitude (z), airspeed (V), and sideslip angle (β). The boundary conditions for the flightpath variables are defined as shown in table 1. A polynomial curve fit of the flightpath state variables is then performed for each of the three flightpath segments. The equations shown for the boundary conditions in table 1 are used to ensure that a smooth, continuous curve results. Care must be taken in defining the boundary conditions so that there are no discontinuities in the higher-order derivatives of the curve fit. If discontinuities exist in, for example, the third derivative of the flightpath heading, a discontinuous control time history will result. This is undesirable because one of the intents of the inverse solution procedure is to produce *natural* control time histories, i.e., control time histories which mimic the control strategy that a pilot would use in performing the same task.

In general, the aircraft equations of motion would be solved simultaneously for the aircraft attitude and control time history. However, the decoupled math model used for this study allows the process to be broken into two steps. First, one solves iteratively for the helicopter attitude, and then solves directly for the control time history. A description of the math model is included in appendix A.

The following iterative process is used at each time step to derive an attitude time history from the polynomial curve fit of the flightpath boundary conditions:

1. Calculate χ, z, V, and β at the new time interval as defined by the polynomial curve fit that was done earlier.

4

2. Transform the flightpath variables into inertial velocities (V_{north}, V_{east}, V_{down}) and inertial accelerations ($\dot{V}_{north}$, $\dot{V}_{east}$, $\dot{V}_{down}$) using the following equations:

$$\gamma = -\sin^{-1}\left(\frac{\dot{z}}{V}\right) \tag{1}$$

$$\dot{\gamma} = \frac{\dot{V}\dot{z} - V\ddot{z}}{V^2 \cos\gamma} \tag{2}$$

$$V_{north} = V \cos\gamma \cos\chi \tag{3}$$

$$V_{east} = V \cos\gamma \sin\chi \tag{4}$$

$$V_{down} = \dot{z} = -V \sin\gamma \tag{5}$$

$$\dot{V}_{north} = \dot{V} \cos\gamma \cos\chi - V\dot{\gamma} \sin\gamma \cos\chi - V\dot{\chi} \cos\gamma \sin\chi \tag{6}$$

$$\dot{V}_{east} = \dot{V} \cos\gamma \sin\chi - V\dot{\gamma} \sin\gamma \sin\chi + V\dot{\chi} \cos\gamma \cos\chi \tag{7}$$

$$\dot{V}_{down} = \ddot{z} = -\dot{V} \sin\gamma - V\dot{\gamma} \cos\gamma \tag{8}$$

3. Make an initial guess at ϕ and θ. This is done either by using the previous values or by extrapolating from a second-order curve fit of the previous three time intervals.

4. Calculate ψ using ϕ, θ, β and the inertial velocities:

$$a_1 \cos\psi + b_1 \sin\psi + c_1 = 0 \tag{9}$$

where

$$a_1 = V_{north} \sin\phi \sin\theta + V_{east} \cos\phi$$

$$b_1 = -V_{north} \cos\phi + V_{east} \sin\phi \sin\theta$$

$$c_1 = V_{down} \sin\phi \cos\theta - V \sin\beta$$

5. Transform the inertial translation and rotational rates and accelerations into the body axis rates and accelerations ($u, v, w, \dot{u}, \dot{v},$ and $\dot{w}$) and the rotational rates ($p, q,$ and r) using ϕ, θ, ψ and the inertial velocities.

6. Solve the equations of motion (eqs. (A5) and (A29)) for new values of ϕ and θ.

7. Check for convergence between these new values of ϕ and θ and the guessed values. If they have not converged sufficiently, repeat steps 4–6 until they do converge.

8. Calculate the body axis angular accelerations. Finally, solve the remaining body axis force and moment equations (eqs. (A1), (A25), (A30), and (A7)) for the control time histories.

To obtain the maximum maneuvering performance of a particular configuration, one iterates on the task boundary conditions until some aircraft limit is reached. In the case of the 180-degree turn, the time to roll in and roll out of the maneuver (which are the same) and the total time to complete the maneuver are adjusted until both the lateral cyclic and the collective inputs reach their travel limits.

Table 1. Boundary conditions for the 180-degree turn

Variable	Point 0	Point 1	Point 2	Point 3
t	0	t_{in}	$t_f - t_{in}$	t_f
χ	0	$\dfrac{\chi_f t_{in}}{2(t_f - t_{in})}$	$\dfrac{\chi_f(2t_f - 3t_{in})}{2(t_f - t_{in})}$	χ_f
$\dot{\chi}$	0	$\dfrac{\chi_f}{t_f - t_{in}}$	$\dfrac{\chi_f}{t_f - t_{in}}$	0
$\ddot{\chi}$	0	0	0	0
$\dddot{\chi}$	0	0	0	0
V	V_i	$\dfrac{-3t_{in}V_i + t_{in}V_f + 2t_f V_i}{2(t_f - t_{in})}$	$\dfrac{t_{in}V_i - 3t_{in}V_f + 2t_f V_f}{2(t_f - t_{in})}$	V_f
$\dot{V}$	0	$\dfrac{V_f - V_i}{t_f - t_{in}}$	$\dfrac{V_f - V_i}{t_f - t_{in}}$	0
$\ddot{V}$	0	0	0	0
$\dddot{V}$	0	0	0	0
z	z	z	z	z
β	0	0	0	0

t_{in} time to roll in (equal to time to roll out)
t_f total time to perform the turn
χ_f final heading (180°)
V_i initial airspeed
V_f final airspeed
z initial altitude (constant)

Note: Constants $\dot{\chi}$ and $\dot{V}$ are assumed from point 1 to point 2.

Table 2. Experimental variables

Max load factor continuous, transient (g)	Max angular rate q_{max}, p_{max} ($\frac{deg}{sec}$)	Damping (at 1 g) M_q, L_p ($\frac{1}{sec}$)
2.00, 2.50	50, 50	−1.0, −2.5
3.00, 3.75	90, 90	−2.0, −5.0
4.00, 5.00	150, 150	−3.8, −9.5

Possible Shortcomings of the Inverse Solution Technique

One should consider how representative of reality the inverse solution technique really is. It is reasonable to expect that a pilot's control technique might not match the inverse solution control technique. There are several possible reasons for this. One is that a pilot will incur certain overshoots or undershoots that require stabilization inputs for correction. Also, a pilot is required to avoid certain maneuver-limiting phenomena (structural load limits, for example) and therefore leaves some small margin of safety with respect to the true maneuver envelope. The inverse solution analysis allows flight up to the very edge of the limiting phenomena, thus gaining an advantage over the pilot. Another source of inaccuracy is that a pilot may be unwilling to command extreme aircraft attitudes or load factors in close proximity to the ground; the inverse solution has no such limits. Finally, it will be shown later in this paper that the polynomials that are part of the inverse solution procedure do not necessarily reflect the true "optimum" flightpath. Therefore the pilot might, in some cases, perform the maneuver somewhat better than the inverse solution would.

To address these issues and to assess the overall validity of the inverse solution technique, a five-week piloted simulation experiment was conducted. The following sections describe that experiment.

PILOTED SIMULATION EXPERIMENT

To validate and refine the inverse solution technique, a five-week simulation investigation was conducted on the NASA Ames Research Center's (ARC) Advanced Cab and Visual System (ACAB) ground-based simulator. A set of maneuvers was flown with a set of configurations that represented a range of MA, and then the results were compared with those predicted by the inverse solution technique for the same maneuvers and configurations. The piloted simulation experiment is described below.

Configurations

Three configuration variables were used, two to represent maneuverability and one to represent agility. Maneuverability was represented by the maximum load factor capability and the maximum pitch and roll rate capability. Agility was represented by the rate damping (or bandwidth) of the pitch and roll response. A summary of the experimental variables is shown in table 2.

The load factor limits were chosen to reflect current capabilities plus possible future capabilities. Table 2 shows the load factor capability at 85 knots, which was the speed used for the two tasks

7

in which load factor capability was important. The table also shows the transient load factor capability. The load factor envelope was varied by changing the load factor limit values used in calculating Z_{δ_c}. Obviously, 4 g of continuous load factor capability is beyond the limits of current helicopter performance, but it is useful to explore this region for its potential maneuverability benefits.

As with the load factor capabilities, the pitch and roll rate limits were chosen to represent current capabilities plus possible future capabilities. Maximum achievable angular rate was varied through the L_{δ_a} and the M_{δ_e} derivatives. Note that the maximum pitch rate capability always matched the maximum roll rate capability.

The pitch and roll rate damping values were chosen as the other variables were. Rate damping was varied through the L_p and M_q stability derivatives. Table 2 shows the three pitch and roll damping pairs used during this experiment.

Tasks

Three tasks were flown during this experiment: a 180-degree turn, a longitudinal pop-up, and a lateral jink. The following three sections describe these tasks.

180-degree turn– The 180-degree turn was chosen because it exercises three of the control axes in an aggressive manner. Also, this maneuver can be considered representative of some of the aggressive maneuvering required of a modern military helicopter. The maneuver was conducted in the following way. The initial flight condition was steady, level flight at an airspeed of 85 knots at some lateral offset from a roadway. The pilot then initiated a 180-degree constant-altitude turn and tried to complete that turn before crossing the centerline of the roadway (fig. 3). The initial lateral offset distance from the roadway determined the aggressiveness of the task. Table 3 contains the task description and the task performance standards.

To determine the maximum maneuvering performance for a given configuration, the pilot repeated the task at various offset distances until two criteria were met at some minimum offset distance. One criterion was that the maneuver could be completed within the stated performance standards without crossing the centerline of the roadway. The other was that the pilot was operating at his maximum tolerable workload. When these two conditions were met, the data-recording equipment was turned on and the pilot performed the maneuver until two representative runs were recorded.

Longitudinal pop-up– Figure 4 shows the longitudinal pop-up maneuver. The helicopter was initialized in steady, level flight (85 knots, 20 ft) at some distance away from an obstacle. Upon reaching a gate set at a specified distance from the obstacle, the pilot initiated a high-effort vertical pop-up to a height of 120 ft in order to clear the obstacle. After clearing the obstacle, the pilot tried to return the helicopter to straight and level flight with no more than 10 ft of overshoot above the final altitude of 120 ft. The aggressiveness of this task was varied by adjusting the distance between the obstacle and the starting gate. Table 4 contains a detailed task description and the task performance standards for the longitudinal pop-up.

As in the 180-degree turn task, the pilot repeated the task until some minimum distance was found where the pilot felt that the maneuver was barely achievable within the stated performance standards. When these conditions were met, the data-recording equipment was turned on and the pilot performed the maneuver until two representative runs were recorded.

Table 3. Task description and task performance standards for the 180-degree turn

Task description	Desired performance	Adequate performance
1. Maintain straight and level flight at 85 knots		
2. When ready, initiate a 180-degree turn	Maintain altitude within ±30 ft; maintain airspeed above 70 knots	
3. Terminate the turn such that the final flight condition is straight and level	Achieve straight and level flight without overshooting the centerline; final altitude within ±30 ft of initial altitude; final airspeed ≥70 knots	Helicopter must be nearly aligned with the roadway and converging toward a steady, level flight condition in a controlled manner
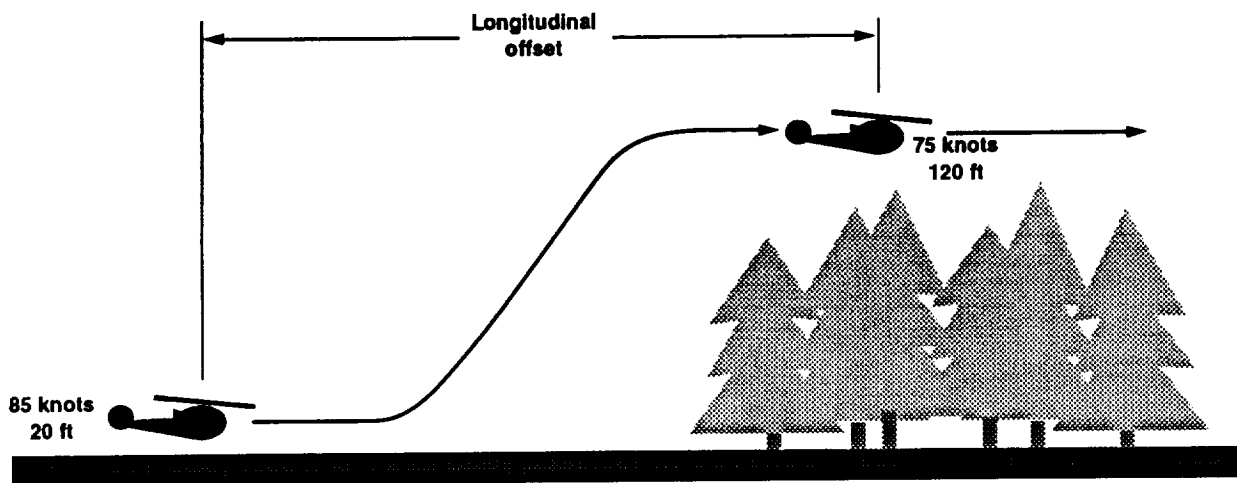
Figure 4. Longitudinal pop-up.

Table 4. Task description and task performance standards for the longitudinal pop-up

Steps	Desired performance	Adequate performance
1. Maintain straight and level flight at 85 knots		
2. Upon reaching the starting gate, initiate a vertical pop-up maneuver to avoid the obstacle	Maintain heading within $\pm 10°$; maintain airspeed within ± 10 knots as the obstacle is cleared	Safely clear the obstacle
3. After clearing the obstacle, return to a steady flight condition at the initial airspeed and an altitude of 120 ft	Return to a stable flight condition at within ± 10 ft of the new altitude; return to within ± 10 knots of the initial airspeed	Helicopter must be positively converging on straight and level flight with safe control of altitude
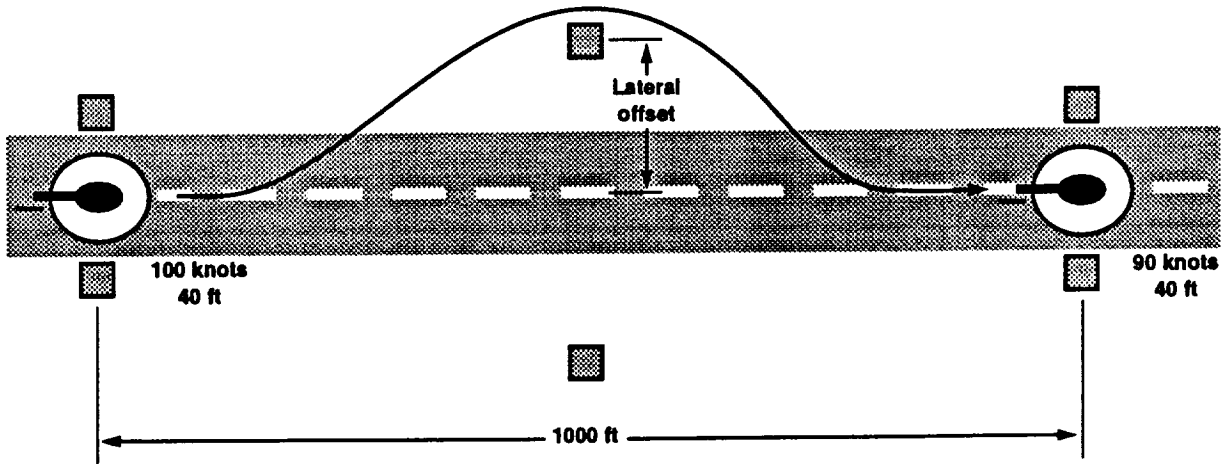
Figure 5. Lateral jink.

Lateral Jink– Figure 5 shows the lateral jink maneuver. The helicopter was initialized in steady, level flight at 100 knots, as shown. As the helicopter approached the first pair of pylons, the pilot was told by a randomized voice command to turn either left or right. After passing through the pylons the pilot initiated a left or right turn (as instructed) in order to fly through the course as shown. After passing around the outer pylon the pilot would maneuver the helicopter so that stable flight was achieved before passing through the final pair of pylons. The aggressiveness of the task was varied by changing the lateral offset distance of the outer pylons. Table 5 contains a detailed task description and the task performance standards for the lateral jink.

As in the other two tasks, the lateral offset distance of the outer pylons was adjusted while the pilot practiced the maneuver until he felt he had achieved maximum performance. When these conditions were met, the data-recording equipment was turned on and two representative runs were completed.

Facility Description

The investigation was conducted using the ARC ACAB facility (fig. 6). The real-time mathematical model was run on an Applied Dynamics AD-100 computer. The visual scene was generated using an Evans and Sutherland CT5 system projected onto the inside of the dome structure. The field of view of the system is ±70 deg horizontally and +45 to –15 deg vertically. Conventional helicopter controls were used; a summary of the force characteristics of the controllers is contained in table 6. Figure 7 shows the simulator cockpit instrument panel. Rotor, engine, and transmission noise were simulated using a Wavetek Helicopter Sound Simulation System.

A seat shaker was used to simulate cockpit vibration. The vibration math model was based on the vibration model developed for a high-fidelity UH-60A Blackhawk simulation (ref. 7). The amplitude and frequency of vibration are calculated as functions of rotor speed, collective stick position, load factor, and airspeed. Extensive tuning of this model was performed during the Blackhawk simulation conducted on the NASA ARC Vertical Motion Simulator facility during June 1989.

11

Table 5. Task description and task performance standards for the lateral jink

Steps	Desired performance	Adequate performance
1. Maintain straight and level flight at 100 knots.		
2. Upon passing through the first gate, initiate either a left or a right turn (as previously instructed) in order to fly safely around the laterally displaced pylon	Maintain airspeed within ±10 knots; maintain altitude within ±10 ft	Maintain safe control of altitude
3. After passing around the pylon, realign the helicopter with the original flightpath and fly through the second gate with wings level	Fly through the second gate in a stable flight condition; maintain airspeed within ±10 knots; maintain altitude within ±10 ft	Pass between the final pair of pylons with safe control of altitude but not necessarily with wings level
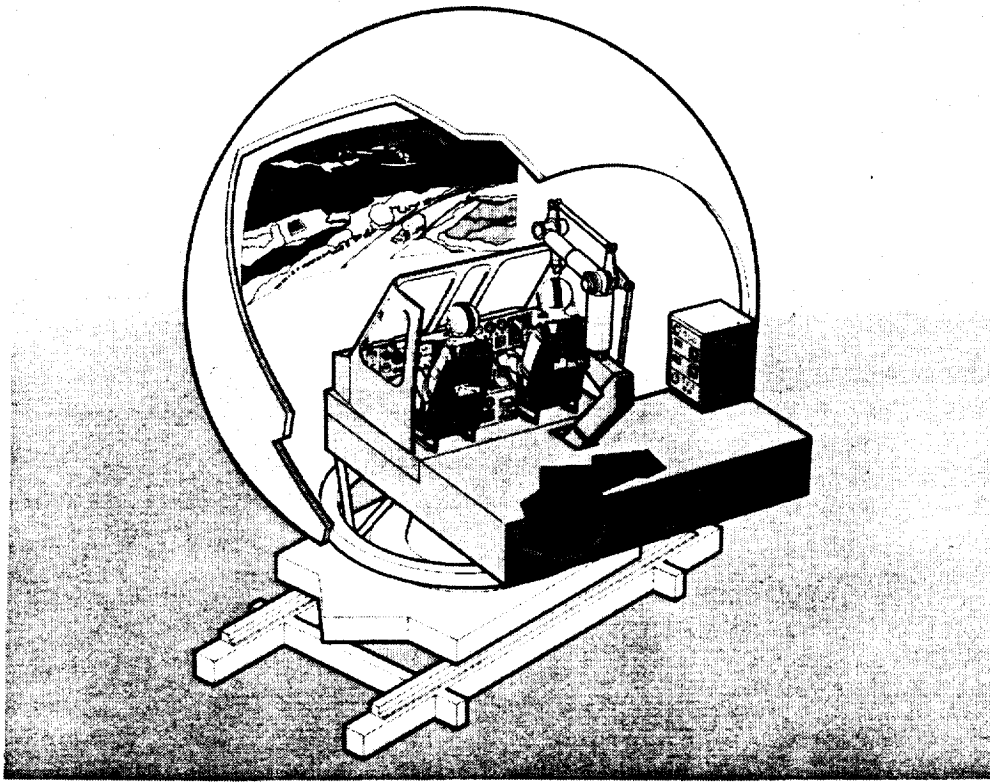
Figure 6. NASA ARC ACAB simulator.

Table 6. Controller characteristics

Axis	Range	Deadzone	Breakout	Gradient	Damping ratio	Friction
	(in)	(in)	(lb)	(lb/in)		(lb)
pitch	±6.15	±.15	1.5	1.5	.8	1.0
roll	±6.10	±.10	1.0	1.0	.5	1.0
yaw	±3.4	±.15	4.0	2.5	1.0	2.0
heave	4.73-10.7	0	0	0	0	3.0
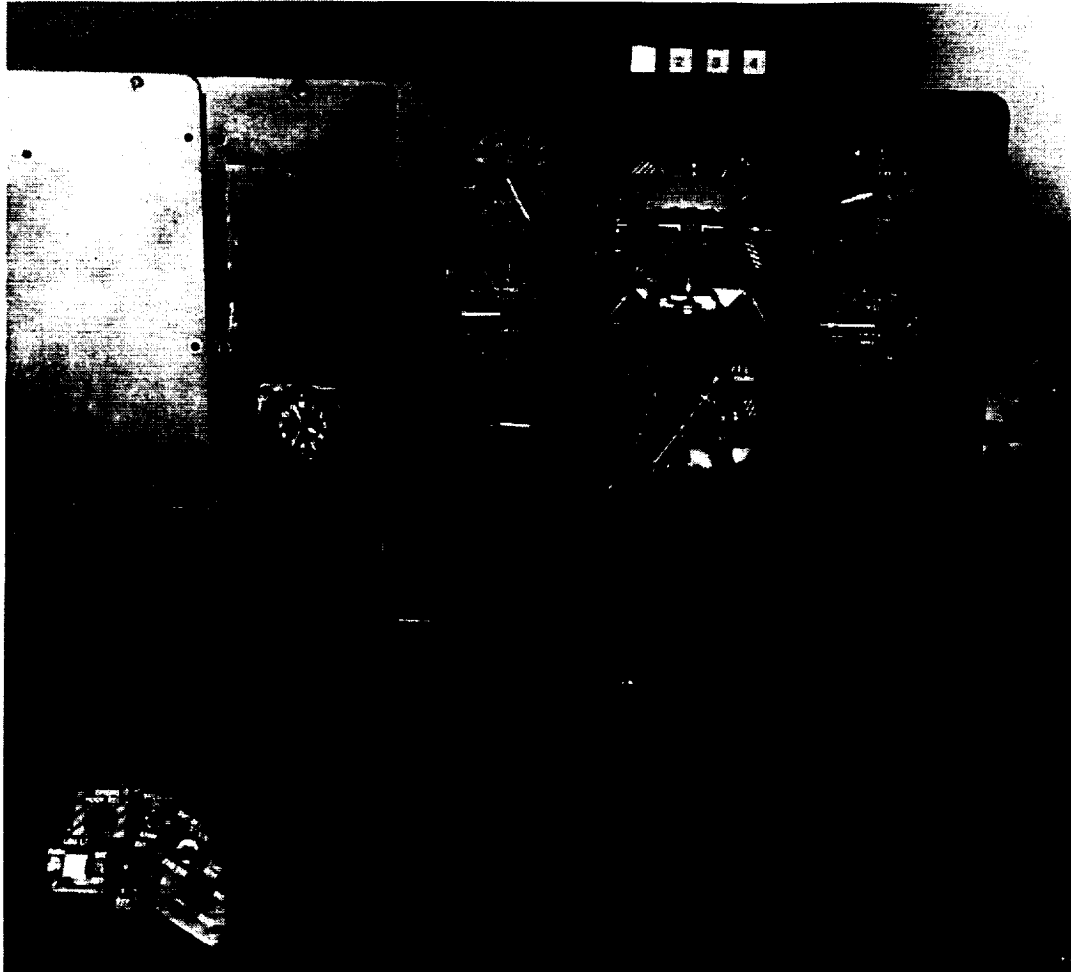
Figure 7. Instrument panel of the simulator cockpit.

Low, medium, and high audio tones indicated to the pilot the helicopter load factors corresponding to 90% maximum continuous, maximum continuous, and maximum transient, respectively. The g meter on the instrument panel, and the seat shaker were additional load factor cues.

Pilots

Six test pilots participated in this experiment. Five were NASA test pilots and one was a U.S. Army test pilot. All of the pilots had extensive rotary-wing experience. No significant difference was seen between the pilots with regard to task performance.

Data Collection

Four types of data were collected. Real-time variables such as position, attitude, and rates were recorded continuously. Performance measures such as maximum track error and maximum heading error were calculated and printed out at the end of each data run. Pilot comments were recorded after each test run. Pilot evaluations in the form of Cooper-Harper ratings (ref. 8) were collected.

RESULTS

In this section, both the inverse solution results and the piloted simulation results will be discussed for each maneuver. The results of the inverse solution will be presented in terms of the variables that are used to define the flightpath, the polynomials that are assumed for those variables, and the actual results of the analysis. The results of the piloted simulation will be discussed in terms of how they relate to the inverse solution results.

180-Degree Turn

Inverse Solution

Inverse Solution Technique– As described previously, the 180-degree turn was broken into three segments: a roll in, a steady turn, and a roll out. The parameters used to define the flightpath are shown with table 1. The total heading change, χ_f, was 180 deg, V_i was set at 85 knots, V_f was set at 70 knots, z was set at 50 ft, and β was held constant at zero. Once these values were defined, the boundary conditions for the maneuver were found using the equations given in table 1. The polynomials assumed for the χ and V equations for each of the three segments were of the form

$$\chi = a_7 t^7 + a_6 t^6 + a_5 t^5 + a_4 t^4 + a_3 t^3 + a_2 t^2 + a_1 t + a_0 \tag{10}$$

$$V = b_7 t^7 + b_6 t^6 + b_5 t^5 + b_4 t^4 + b_3 t^3 + b_2 t^2 + b_1 t + b_0 \tag{11}$$

A seventh-order polynomial is needed to account for the eight boundary conditions of each segment. These equations were then used in the manner discussed earlier to arrive at a solution. The variables t_f and t_{in} were adjusted until both the collective and the lateral stick inputs were maximized. Table 7 lists the values of t_f and t_{in} that were found to maximize these inputs for the 27 different configurations.

15

Table 7. Values at t_f/t_{in} used in evaluating the 180-degree turn

Max pitch and roll rate (deg/sec)	Damping pitch, roll ($\sec^{-1}$)	Load factor capability (g) continuous, transient		
		2,2.5	3,3.75	4,5
50	−1,−2.5	9.15,4.29	8.96,4.48	8.96,4.48
	−2,−5	8.73,3.85	8.36,4.18	8.36,4.18
	−3.8,−9.5	8.58,3.69	8.14,4.07	8.14,4.07
90	−1,−2.5	7.67,2.75	6.87,3.16	6.66,3.33
	−2,−5	7.26,2.31	6.4,2.67	5.96,2.98
	−3.8,−9.5	7.06,2.09	6.18,2.44	5.62,2.81
150	−1,−2.5	6.9,1.94	5.98,2.22	5.24,2.62
	−2,−5	6.53,1.55	5.56,1.78	4.62,2.21
	−3.8,−9.5	6.33,1.34	5.34,1.55	4.34,1.92

Figure 8 shows a typical time history from the inverse solution. The configuration in this case is the medium load factor (3 g continuous), medium roll rate (90 deg/sec), and medium roll damping (−5.0 1/sec). Note that the lateral and collective stick time histories achieve a maximum at the control travel limits of 6.1 and 10.7 in., respectively. Figure 9 shows the flightpath of the same maneuver.

Inverse Solution Results– As stated in the task description, the lateral distance was chosen as the performance measure for this maneuver. Figure 10 shows the results of the inverse solution analysis of the 180-degree turn in terms of the lateral distance required to turn for each configuration. Each symbol on the plot represents a single configuration. There are a total of twenty-seven different configurations because there are low, medium, and high values for each of three configuration variables. The configurations in the figure are grouped in the following ways: configurations with a common load factor capability are connected by a dashed line, and configurations with a common roll rate capability are grouped vertically above the appropriate value shown on the horizontal axis. The damping is indicated by the shading of the symbols.

In general, it can be seen that the load factor capability has the dominant effect on the lateral distance required to turn. There is nearly a 40% difference in performance between the 2-g configurations and the 4-g configurations. It can also be seen that there is little variation with roll rate capability. This is somewhat surprising, as one might expect that the ability to initiate and terminate the maneuver faster would allow more use of the load factor capability, resulting in better performance. The roll damping has little effect on the lateral turn distance. This is because the damping affects only the roll-in and roll-out transient segments and will therefore generally have little effect on the overall performance for this task.

It should be noted that the medium load factor with low roll rate configurations, and the high load factor with medium and low roll rate configurations both yielded solutions in which there was not enough roll rate capability to take full advantage of the load factor capability. That is, half of the maneuver was spent rolling in and half of the maneuver was spent rolling out; the inverse
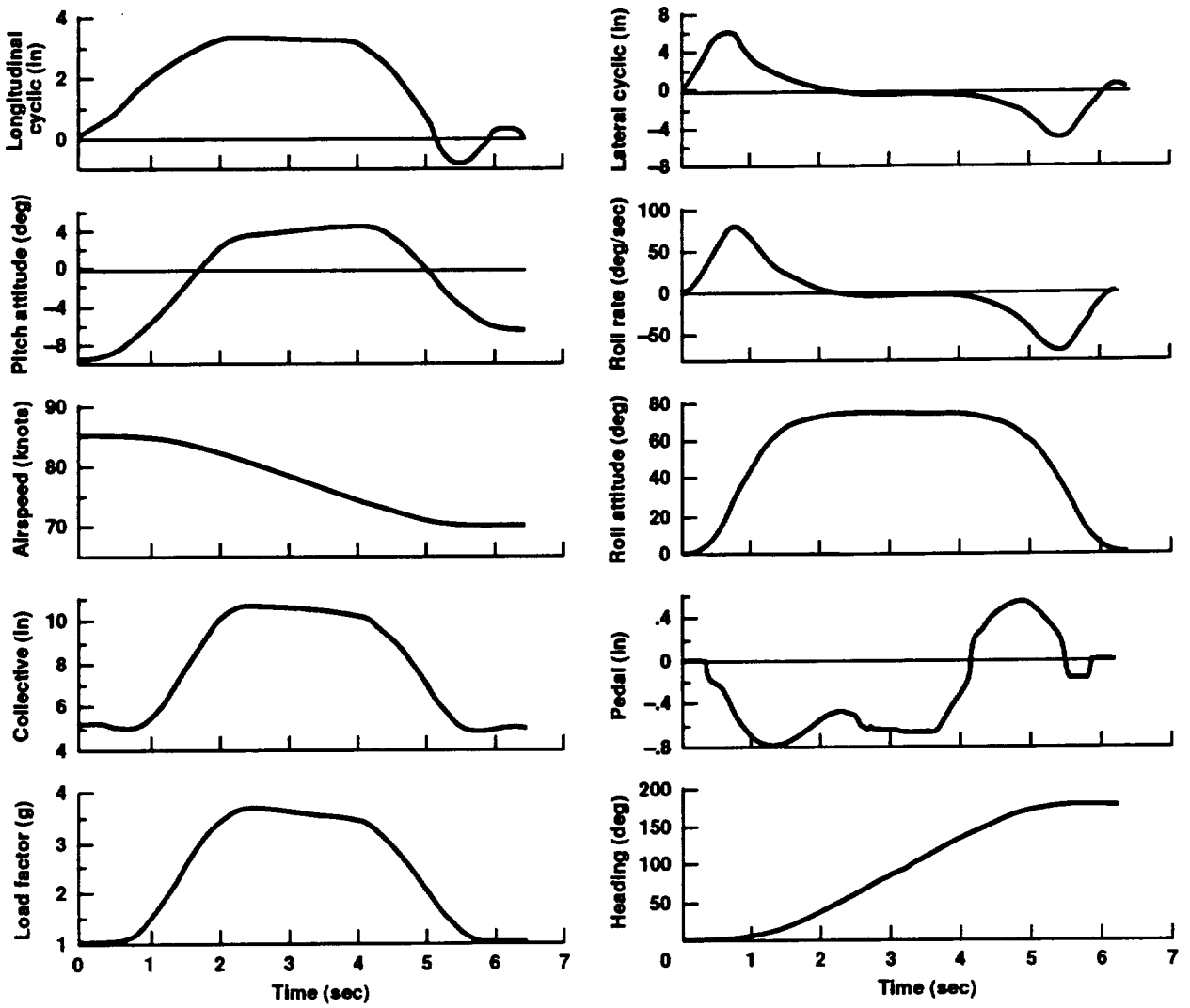
Figure 8. Typical inverse solution state and control time histories for the 180-degree turn.
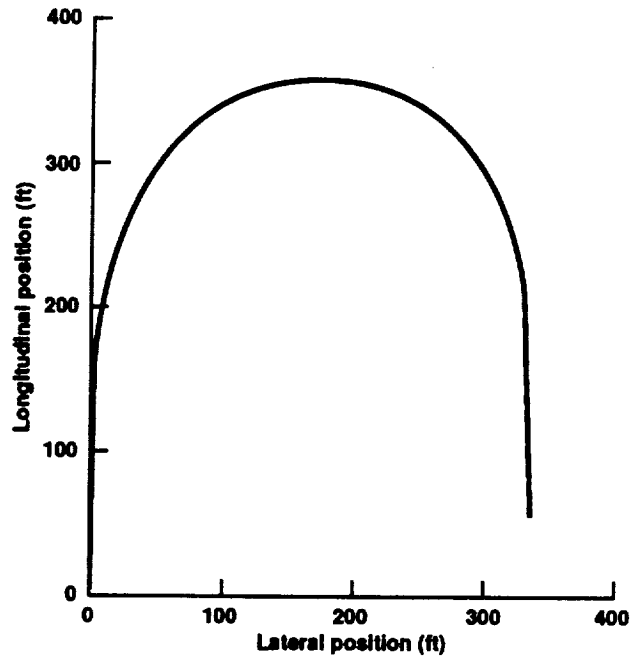
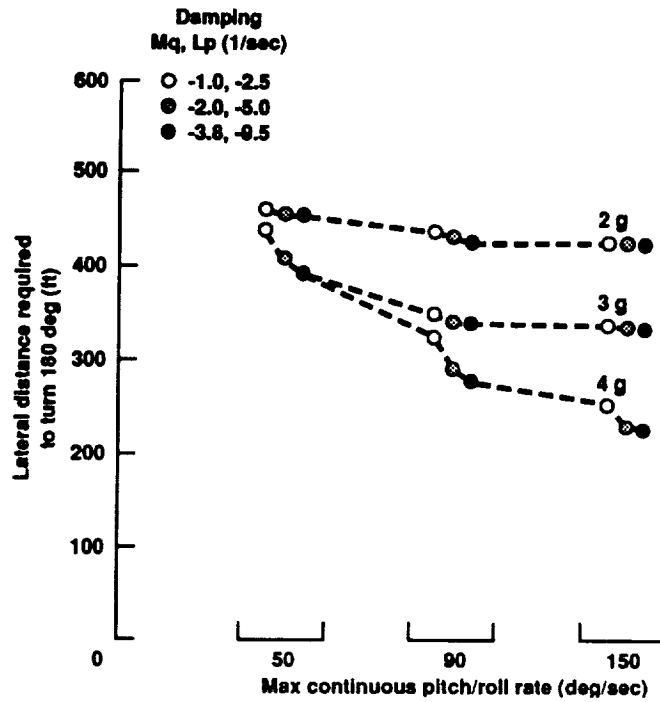Figure 9. Typical inverse solution flightpath for the 180-degree turn.

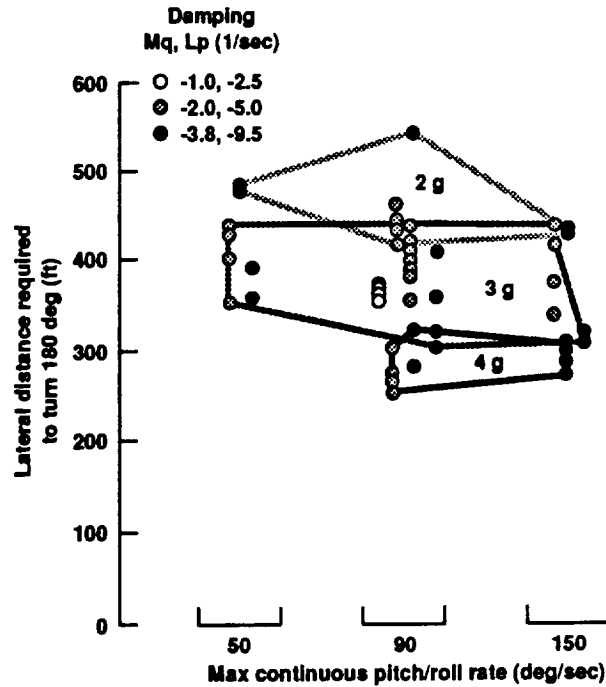Figure 10. Inverse solution results for the 180-degree turn.

Figure 11. Piloted experiment results for the 180-degree turn.

solution was never able to reach the steady-state load factor capability of the configuration and achieve a steady turn rate. It is interesting to observe that when this situation occurs, the effect of bandwidth becomes more significant. This is because such a large portion of the maneuver consists of initiating and terminating the roll angle. The inverse solution technique permits the determination of a balanced MA (load factor and roll rate capability) configuration for this task.

Piloted Simulation Experiment

The piloted results for the 180-degree turn are shown in figure 11. The results are plotted exactly as they were in figure 10 except that each symbol represents an individual run. The common load factor configurations are grouped by the envelopes shown, the common roll rate configurations are grouped vertically above the appropriate value shown on the horizontal axis, and the damping is indicated by the shading of the symbol.

One can immediately see the same trends that existed for the inverse solution. That is, the load factor capability of the configuration has the dominant effect on performance, there is little improvement in performance with increased roll rate capability, and the damping is of almost no consequence.

Figure 12 shows an overlay of the inverse solution results and the piloted experiment results. There is general agreement between them. For this maneuver, the inverse solution technique yields reasonably accurate results.

A series of roll-angle time history plots is presented to illustrate that the roll rate limiting phenomenon described in the previous section manifested itself during the piloted experiment. Figure 13 shows those cases where the configuration had a maximum roll rate capability of 150 deg per sec, a medium (3-g) continuous load factor capability, and medium (−5.0-1/sec) roll damping.
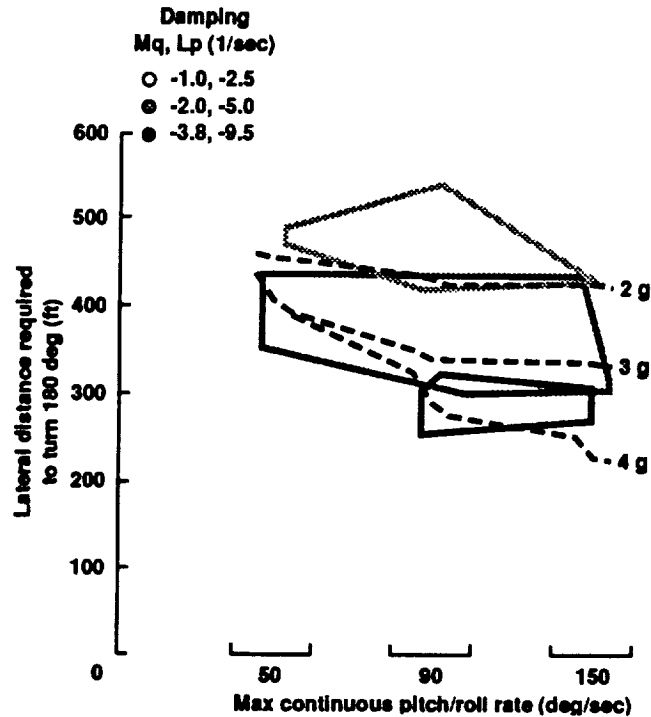
19

Figure 12. Piloted experiment and inverse solution results for the 180-degree turn.

Figure 14 shows those configurations which had a roll rate capability of 90 deg per sec and the same continuous load factor and damping. Figure 15 contains those configurations with a 50-deg-per-sec roll rate capability and the same continuous load factor and roll rate capability. Clearly, the high-roll-rate configuration plot shows that the pilot was able to set a bank and maintain a steady turn during a portion of the maneuver. The medium-rate plot shows the same effect but to a lesser degree. The low-roll-rate plot begins to show the limiting effects of the roll rate capability; the pilot is spending nearly all of the time either rolling in or rolling out.

Figure 16 shows the Cooper-Harper pilot ratings for the piloted experiment. Each symbol represents one pilot's rating of a particular configuration. For clarity, the three load factor configurations are shown on three different plots. It can be seen that no significant trend exists in the pilot rating data. This was because, as part of the experiment procedure, the task setup (in this case the lateral offset distance) was adjusted until the pilot felt that borderline desired performance was achieved. This resulted in pilot opinion being naturally driven toward a Cooper-Harper rating of four. Variations from a rating of four occurred when the pilot felt that a configuration was particularly responsive and predictable or particularly sluggish and unpredictable. An attempt was made to eliminate these variations by increasing or decreasing the lateral offset difference, but variations occurred nevertheless. It should be noted that after the pilots were allowed to practice the maneuver, variation between pilots in offset distance was minimal.
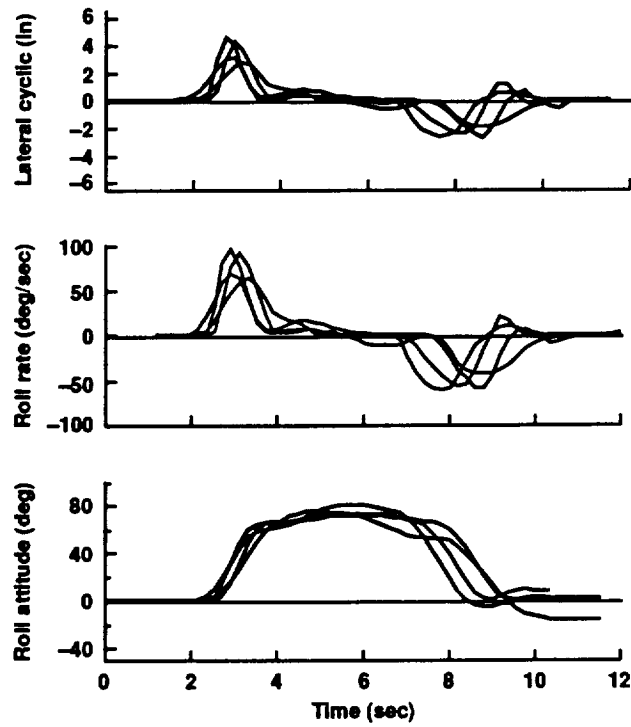
20

Figure 13. Roll attitude, roll rate, and lateral cyclic versus time (150-deg/sec roll rate configurations).
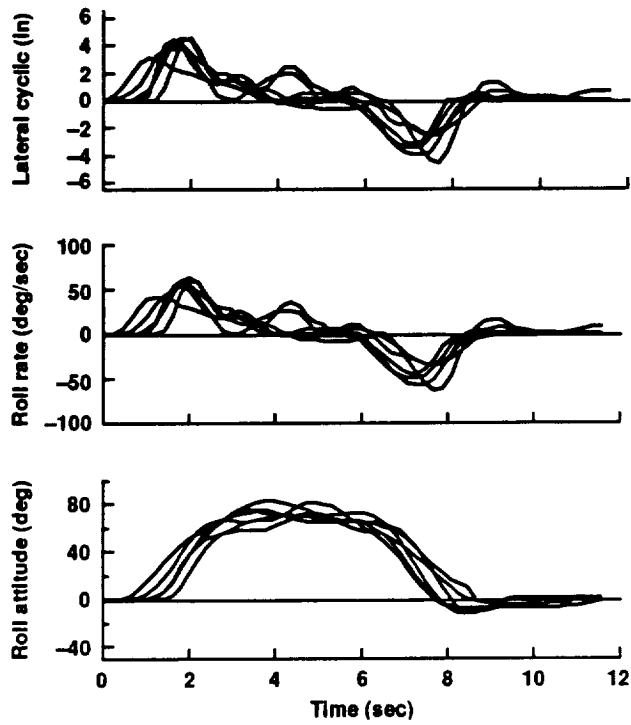

Figure 14. Roll attitude, roll rate, and lateral cyclic versus time (90-deg/sec roll rate configurations).
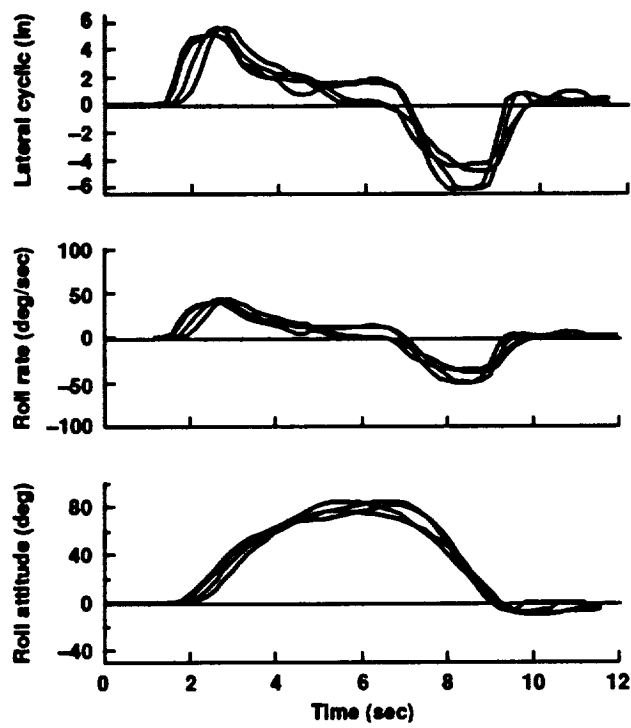
Figure 15. Roll attitude, roll rate, and lateral cyclic versus time (50-deg/sec roll rate configurations).
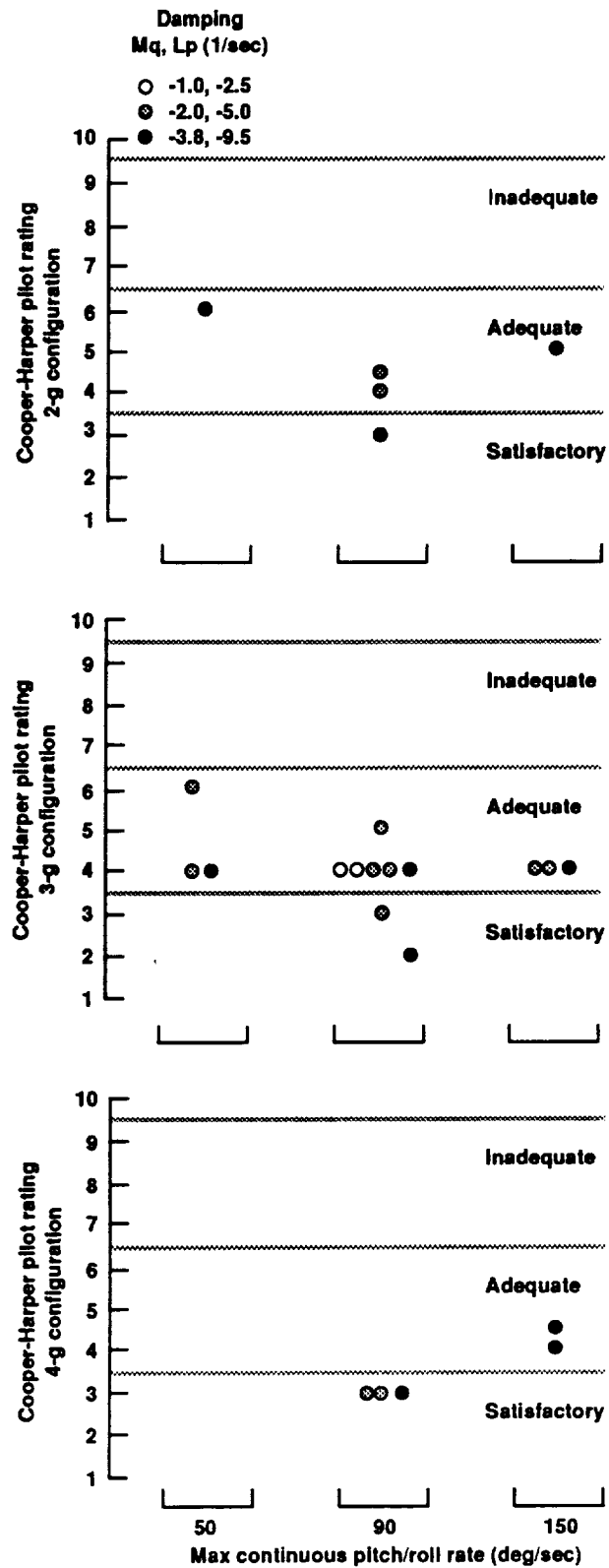
Figure 16. Cooper-Harper pilot ratings for the 180-degree turn.

Longitudinal Pop-Up

Inverse Solution

Inverse Solution Technique– For the longitudinal pop-up maneuver, the pitch attitude, θ, has been used as a flightpath descriptor. This is because if airspeed is used as the flightpath descriptor, wildly varying pitch attitude profiles can result. For relatively small changes in the airspeed profile, drastically different pitch attitude time histories can result, if a solution can be reached at all. The solution procedure then is to trim the model at the desired initial airspeed, and then allow it to vary as the pitch attitude proceeds through its specified time history. By altering the pitch attitude time history, the desired final airspeed can be attained. This is analogous to what the pilot would do, i.e., the primary control loop for the pilot in this case is the pitch attitude.

The parameters used to define the longitudinal pop-up maneuver are

> total time to perform the maneuver, t_f
>
> initial/final altitude, z_i, z_f
>
> peak attitude change, $\Delta\theta$
>
> initial/final airspeed, V_i, V_f
>
> flightpath heading, χ
>
> sideslip angle, β

Initial altitude, z_i, was set at 20 ft, z_f was set at 120 ft, V_i was set at 85 knots, V_f was set at 75 knots, and flightpath heading and sideslip angle were both held constant at zero. As was stated previously, the peak attitude change was adjusted to arrive at the desired final airspeed. Once these values were set, the boundary conditions for the maneuver were set in accordance with table 8. The polynomials used are of the form

$$z = a_9t^9 + a_8t^8 + a_7t^7 + a_6t^6 + a_5t^5 + a_4t^4 + a_3t^3 + a_2t^2 + a_1t + a_0 \tag{12}$$

$$\theta = b_{10}t^{10} + b_9t^9 + b_8t^8 + b_7t^7 + b_6t^6 + b_5t^5 + b_4t^4 + b_3t^3 + b_2t^2 + b_1t + b_0 \tag{13}$$

where the order of the polynomials is selected so that the unknown coefficients can be determined uniquely with the boundary conditions shown in table 8. These equation were then used, in the manner previously described, to arrive at a solution that provides both the correct final airspeed and maximization of the collective input. Table 9 lists the values of t_f and t_i that were found to maximize the collective and lateral inputs.

Figure 17 shows a typical time history from the inverse solution. The configuration in this case is the medium load factor (3 g continuous), medium pitch rate (90 deg/sec), and medium pitch damping (–2.0 1/sec). Note that the collective stick achieves a maximum at the control travel limits of 10.7 in. Also note that the longitudinal stick displacement required to induce the 10-knot airspeed loss is far less than the maximum travel available. Figure 18 shows a profile view of the flightpath of the same maneuver.

Inverse Solution Results– The performance criterion that was chosen for the longitudinal pop-up was the total longitudinal distance required to perform the maneuver. Figure 19 shows the

Table 8. Boundary conditions for the longitudinal pop-up

Variable	Point 1	Point 2	Point 3
t	0	$t_f/2$	t_f
z	z_i	unconstrained	z_f
$\dot{z}$	0	unconstrained	0
$\ddot{z}$	0	unconstrained	0
$\dddot{z}$	0	unconstrained	0
$\ddddot{z}$	0	unconstrained	0
θ	θ_{trim}	$\theta_{\text{trim}} + \Delta\theta$	θ_{trim}
$\dot{\theta}$	0	unconstrained	0
$\ddot{\theta}$	0	unconstrained	0
$\dddot{\theta}$	0	unconstrained	0
$\ddddot{\theta}$	0	unconstrained	0
χ	0	0	0
β	0	0	0

Table 9. Values of t_f and $\Delta\theta$ used in evaluating the longitudinal pop-up

| Max pitch and roll rate (deg/sec)	Damping pitch, roll (sec^{-1})	Load factor capability (g) continuous, transient		
		2,2.5	3,3.75	4,5
50	−1,−2.5	5.14,17.28	4.03,21.2	3.33,18.56
	−2,−5	5.14,17.28	4.03,21.2	3.33,18.56
	−3.8,−9.5	5.14,17.28	4.03,21.2	3.29,18.5
90	−1,−2.5	5.14,17.28	4.03,21.2	3.44,24.2
	−2,−5	5.14,17.28	4.03,21.2	3.44,24.2
	−3.8,−9.5	5.14,17.28	4.03,21.2	3.44,24.2
150	-1,-2.5	5.14,17.28	4.03,21.2	3.44,24.2
	-2,-5	5.14,17.28	4.03,21.2	3.44,24.2
	-3.8,-9.5	5.14,17.28	4.03,21.2	3.44,24.2
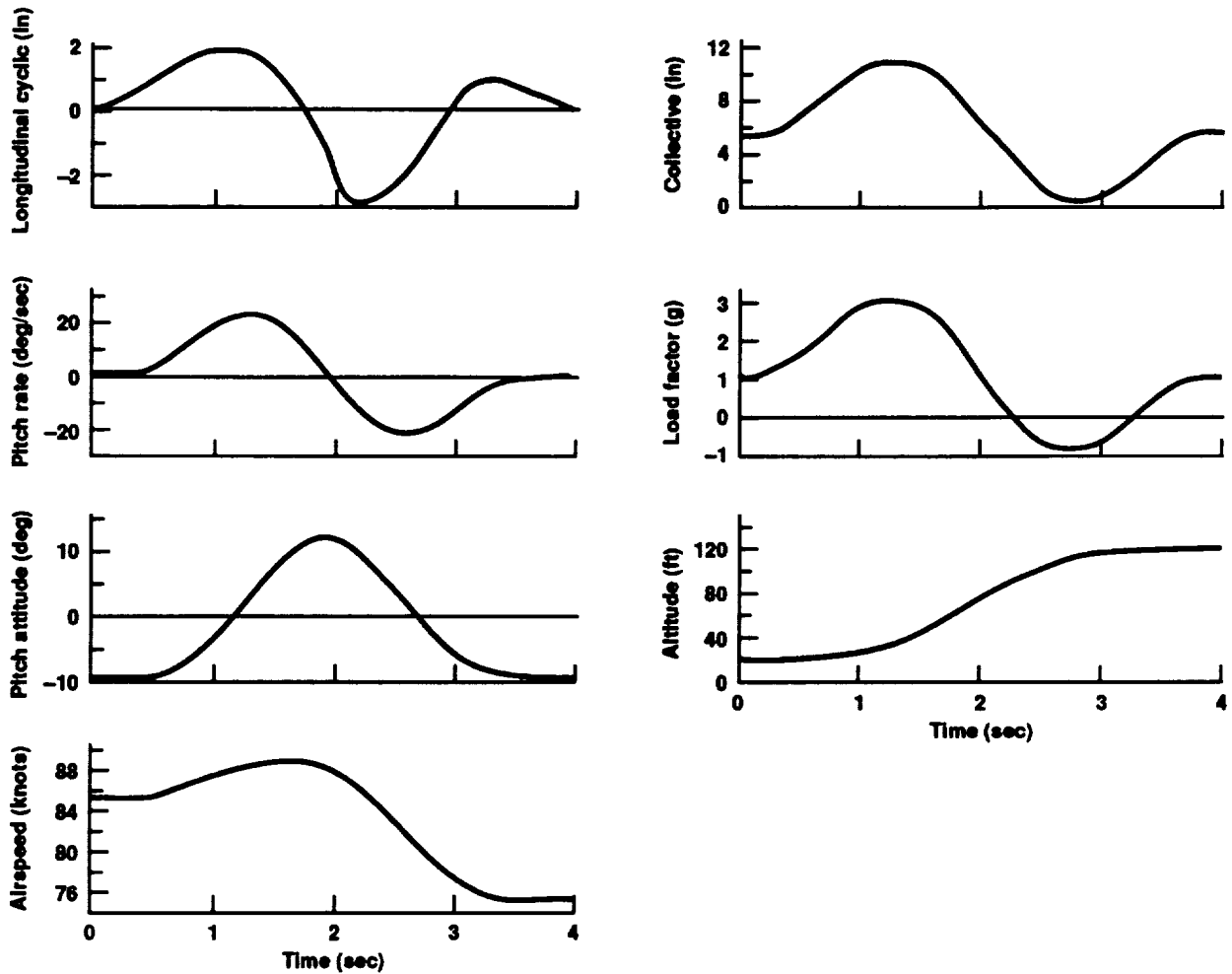
Figure 17. Typical time history of the inverse solution of the longitudinal pop-up.
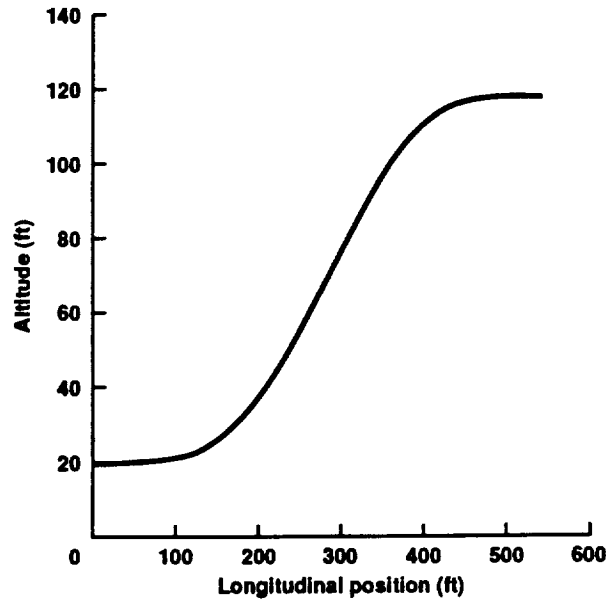
Figure 18. Typical flightpath of the inverse solution of the longitudinal pop-up.

results of the inverse solution analysis in terms of the total longitudinal distance required. Note that the pitch control power and pitch damping have no effect on the inverse solution results for this maneuver, because the maximum pitch rate required for the maneuver is much less than 50 deg/sec, as shown in figure 18. It can be seen that the load factor capability dominates the performance.

Piloted Simulation Experiment

The piloted results for the longitudinal pop-up maneuver are shown in figure 20. The results are plotted exactly as they are in figure 19 except that each symbol represents an individual run. Also, the dashed lines which connect the common load factor configurations in figure 19 are overlaid on figure 20. Only those configurations with the medium pitch damping were examined during the piloted simulation experiment.

For the configurations with the 3- and 4-g load factor capability, there is general agreement between the inverse solution analysis and the piloted simulation data. For the configurations with the 3-g load factor capability, the pitch rate capability had little influence on performance as predicted by the inverse solution. However, the inverse solution results for the 2-g load factor case appear to be slightly conservative when compared with the piloted results.

The primary reason for the difference between the inverse solution results and the piloted results for the 2-g case is the fact that the pilots tended to command a more rapid pitch input in the beginning of the maneuver, which resulted in a more rapid airspeed reduction and therefore a shorter distance to perform the maneuver. This can be seen in figure 21, which is a co-plot of results from a typical piloted run with those of the inverse solution for the 2-g configuration.

Figure 22 shows the Cooper-Harper pilot ratings for the longitudinal pop-up. As with the 180-degree turn task, the ratings were all in the vicinity of four. Again, the reason for this is that the pilots were allowed to adjust the task performance measure (longitudinal distance, in this case) until they felt that they were just barely achieving desired performance.
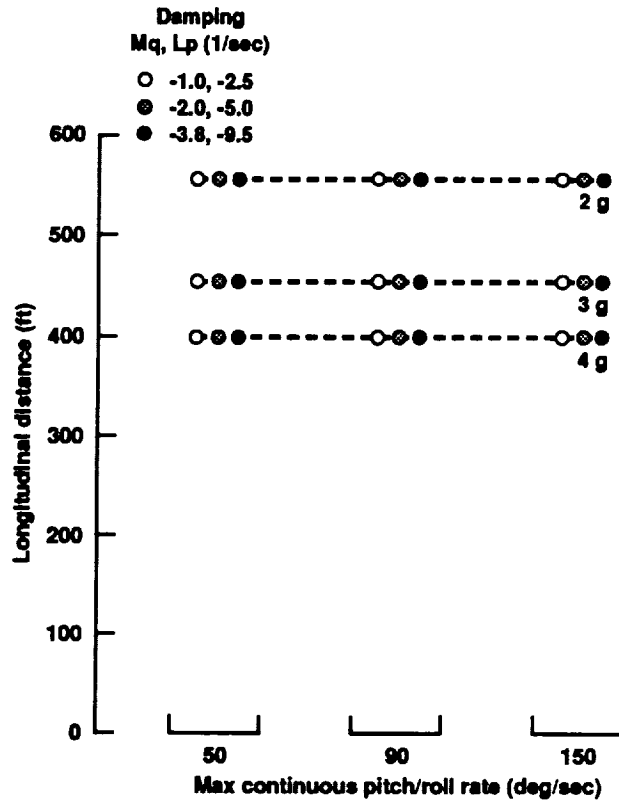
27

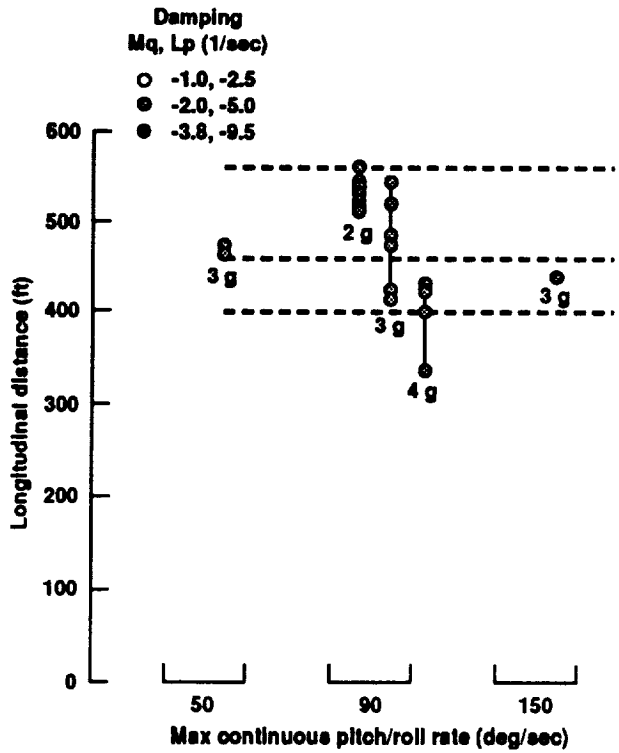Figure 19. Inverse solution results for the longitudinal pop-up.

Figure 20. Piloted experiment and inverse solution results for the longitudinal pop-up.
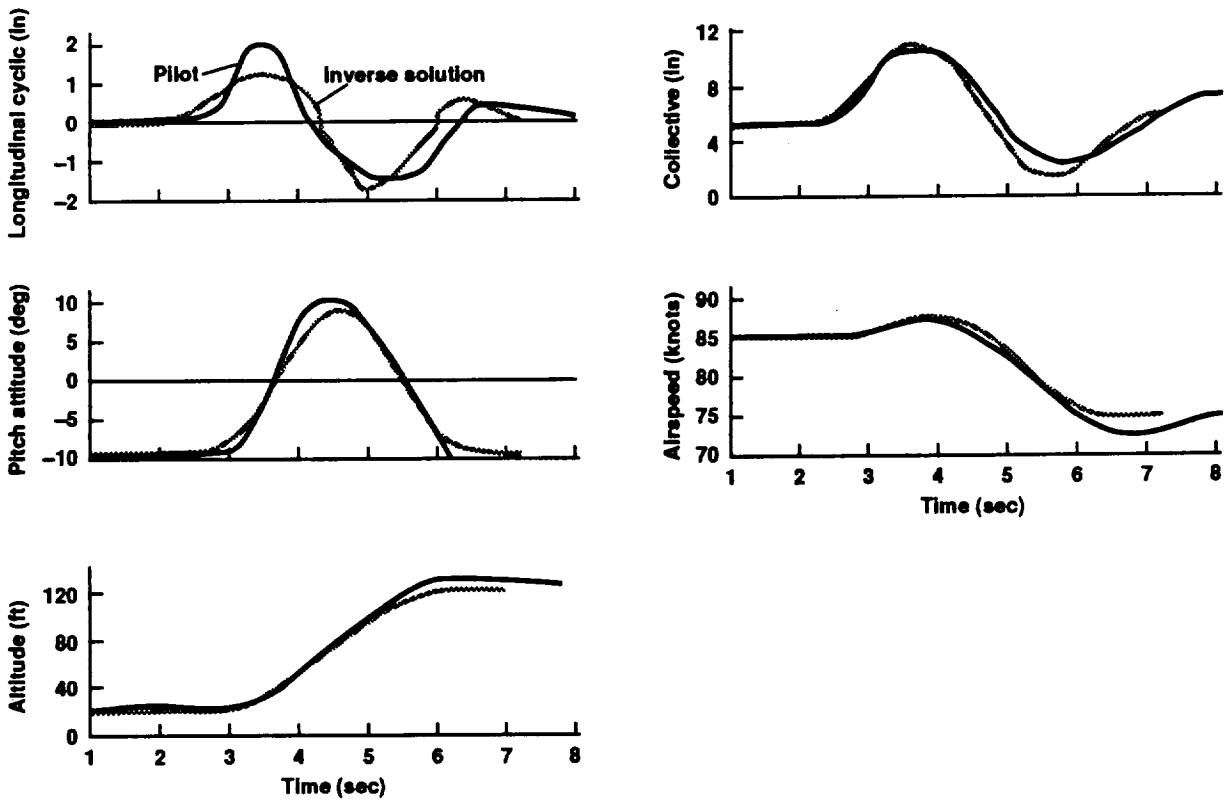
Figure 21. Time history of a typical piloted longitudinal pop-up versus the inverse solution for the 2-g load factor case.
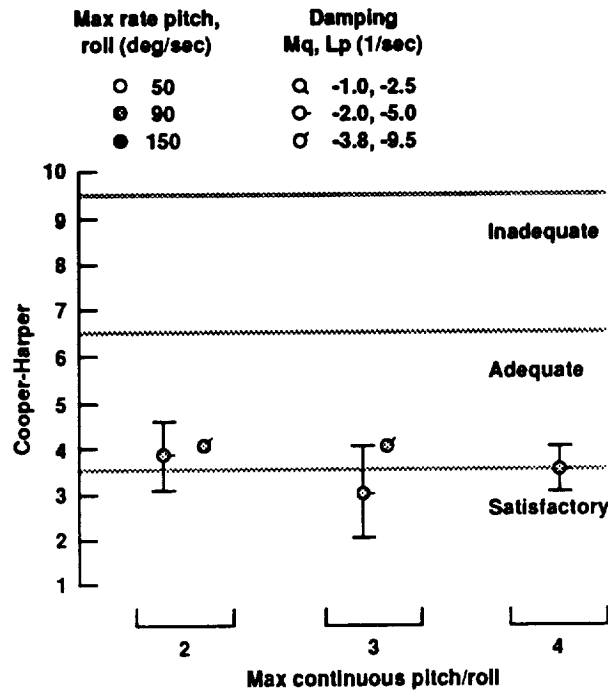

Figure 22. Cooper-Harper pilot ratings for the longitudinal pop-up.

Table 10. Boundary conditions for the lateral jink

Variable	Point 1	Point 2	Point 3
t	0	$t_f/2$	t_f
χ	0	0	0
$\dot{\chi}$	0	$\dot{\chi}_1$	0
$\ddot{\chi}$	0	unconstrained	0
$\dddot{\chi}$	0	unconstrained	0
z	h_{ic}	h_{ic}	h_{ic}
$\dot{z}$	0	0	0
$\ddot{z}$	0	0	0
$\dddot{z}$	0	0	0
V	V_{ic}	V_{ic}	V_{ic}
$\dot{V}$	0	0	0
$\ddot{V}$	0	0	0
β	0	0	0
$\dot{\beta}$	0	0	0
$\ddot{\beta}$	0	0	0
$\dddot{\beta}$	0	0	0

Lateral Jink

Inverse Solution

The parameters used to define the lateral jink were

altitude, h_{ic}
airspeed, V_{ic}
longitudinal distance of the maneuver, $x_{distance}$
lateral distance of the maneuver, $y_{distance}$

For this maneuver, the total time and the $\dot{\chi}_1$ needed to match the longitudinal and lateral maneuver distances were determined iteratively. The boundary conditions were defined as shown in table 10. Table 11 lists the values used in the analysis. The polynomial assumed for χ was

$$\chi = a_7 t^7 + a_6 t^6 + a_5 t^5 + a_4 t^4 + a_3 t^3 + a_2 t^2 + a_1 t + a_0 \tag{14}$$

and the remaining flightpath descriptors

$$z = h_{ic} \tag{15}$$

$$V = V_{ic} \tag{16}$$

$$\beta = 0 \tag{17}$$

The lateral jink was analyzed for the configurations that were used during this experiment, and the results are shown in figure 23. The results of the inverse solution show no variation with collective control power and only small variations with roll damping. The configurations with 150-deg/sec roll rate capability have nearly twice the performance as the configurations with a 50-deg/sec roll rate capability in terms of the lateral offset achievable.

30

Table 11. Values of χ_1 and t_f used in evaluating the longitudinal pop-up

| Max pitch and roll rate (deg/sec)	Damping pitch, roll (sec^{-1})	Load factor capability (g) continuous, transient		
		2,2.5	3,3.75	4,5
50	−1,−2.5	5.43,5.94	5.43,5.94	5.43,5.94
	−2,−5	5.68,5.94	5.68,5.94	5.68,5.94
	−3.8,−9.5	5.82,5.94	5.82,5.94	5.82,5.94
90	−1,−2.5	9.39,5.94	9.39,5.94	9.39,5.94
	−2,−5	10.54,5.94	10.54,5.94	10.54,5.94
	−3.8,−9.5	11.34,5.94	11.34,5.94	11.34,5.94
150	-1,-2.5	14.5,5.94	14.5,5.94	14.5,5.94
	-2,-5	16.41,5.96	16.41,5.96	16.41,5.96
	-3.8,-9.5	18.04,5.98	18.04,5.98	18.04,5.98
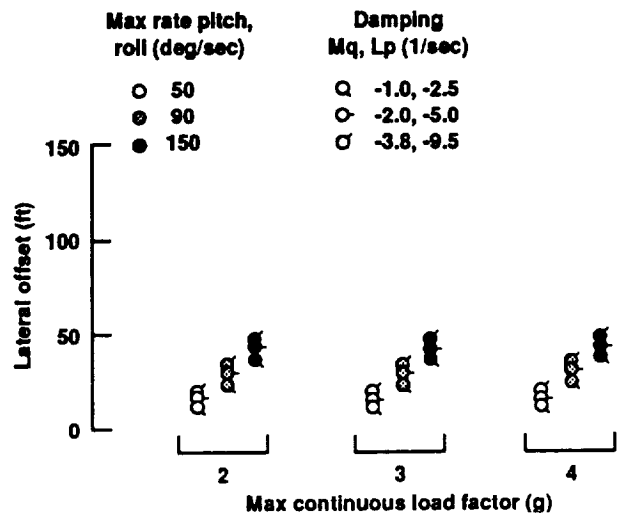
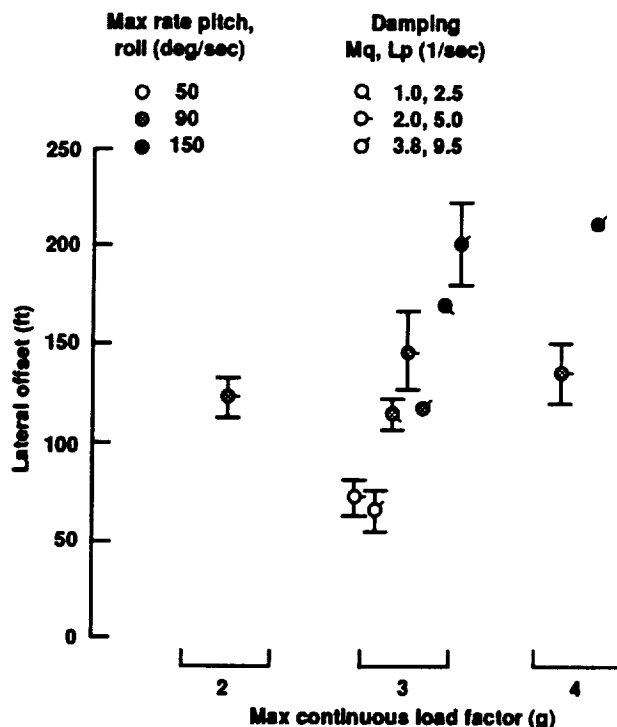Figure 23. Inverse solution results for the lateral jink.

Figure 24. Piloted experiment results for the lateral jink.

Piloted Simulation Experiment

The piloted results for the longitudinal pop-up maneuver are shown in figure 24. The results are plotted exactly as they were in figure 23, except that each symbol represents the average of the runs made with that configuration and the bars represent the standard deviation.

On first inspection, the piloted results seem to indicate that the performance estimates made using the inverse solution are grossly conservative. However, if one examines time histories of the pilots flying the maneuver as compared to the inverse solution, it becomes clear that the pilots were flying the maneuver quite differently than was assumed for the inverse solution.

Figure 25 shows plots of lateral stick, roll angle and lateral position versus x-position for both the inverse solution and for five runs made by three pilots (L_p equals -5.0, maximum roll rate equals 90 deg/sec). It can be seen that the pilots were passing through the final gate (1,000 ft) with an average roll angle of 40 deg, as opposed to the inverse solution assumption of steady level flight by the same point. This resulted from a failure to make clear to the pilots that they were to achieve steady level flight before passing through the final gate. It should be noted, however, that the inputs that result from the inverse solution do resemble the pilot inputs for the same maneuver.

Finally, the piloted results do show both the improved performance with increasing roll control power and the lack of performance change with collective control power that was seen in the inverse solution results. Also, the Cooper-Harper pilot ratings fell just inside the Level 2 region, as expected, because the pilots were flying the maneuver to what they felt to be their maximum level of aggressiveness (fig. 26).
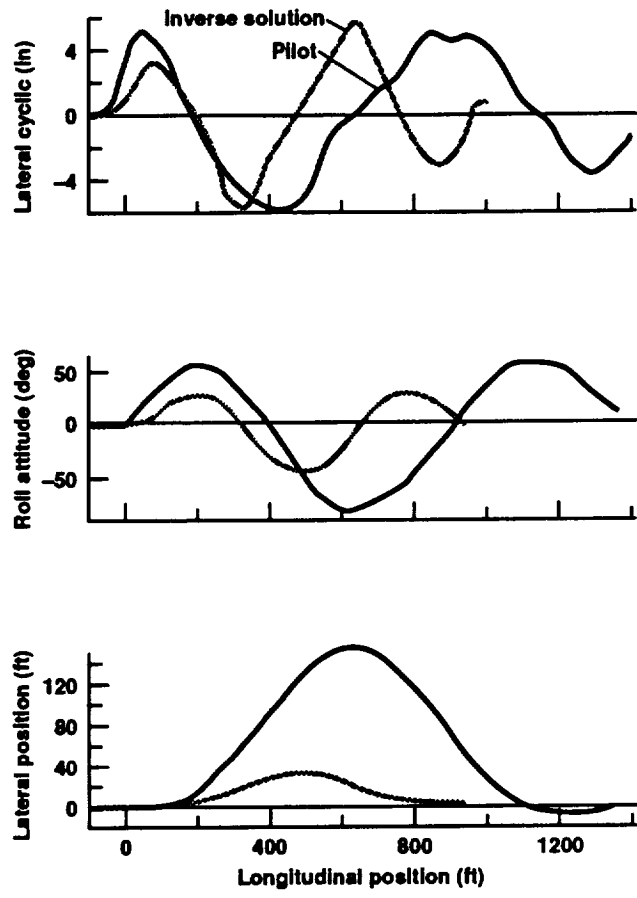
32

Figure 25. Lateral stick, roll attitude, and lateral position versus longitudinal position for the lateral jink.
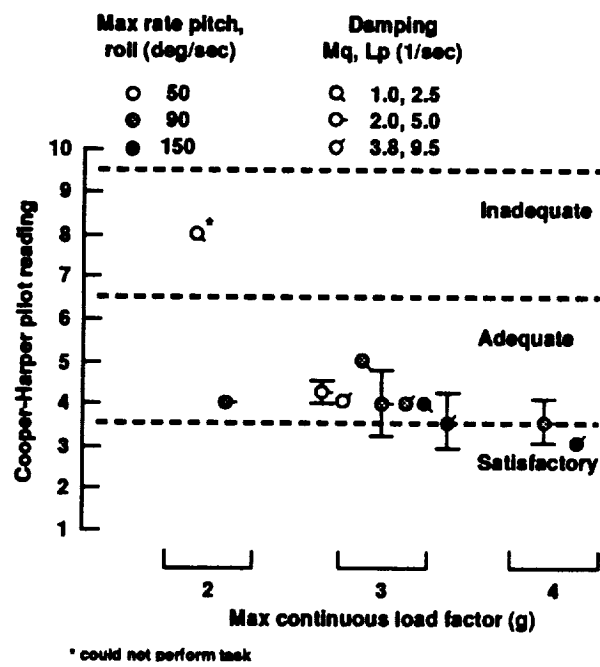
Figure 26. Cooper-Harper pilot ratings for the lateral jink.

CONCLUDING REMARKS

Two things separate this inverse solution study from previous work in the same area. First, in this study, the inverse solution technique was used to determine the *maximum* maneuvering capability of a given MA configuration using "pilotlike" control inputs. That is, the flightpath definitions were varied until maximum control authority was used, but with the constraint that the control inputs had to be smooth and continuous. Second, extensive pilot-in-the-loop simulation data was gathered in order to determine whether the inverse solution was valid.

In general, for the three maneuvers described, the inverse solution could be easily made to generate the desired flightpaths with smooth control inputs. Numerical convergence was rapid, and very few difficulties were encountered in reaching a solution once a polynomial representation of the flightpath had been established. For the 180-degree turn and the longitudinal pop-up the technique yielded accurate predictions of what the pilot could be expected to perform. For the lateral jink, the inverse solution results did not match the piloted simulation results, but this was because the pilots were flying the maneuver in a different manner.

For the three maneuvers examined during this experiment, the inverse solution technique correctly predicted the relative effects that the various MA parameters had on maneuvering performance. For the 180-degree turn, the MA variable that dominated performance was the load factor capability, whereas the roll rate and damping had little effect. For the longitudinal pop-up, the load factor capability dominated performance. For the lateral jink, the roll rate capability dominated performance and the load factor capability and roll damping had little effect.

It was not demonstrated that being close to the ground or close to an aircraft limit had any effect on the pilot's willingness to make full use of the maneuvering envelope. Pilot commentary indicates that this was because the maneuvers were flown repeatedly, which resulted in a high level of pilot proficiency and comfort. Also, because the simulator posed no threat of an accident, the pilots tended to make use of all of the maneuver envelope available to them.

It is important to point out that, although the aim of this technique was to find the maximum performance that could be achieved by a pilot, the technique does not result in the "optimum" performance. To achieve the optimum solution one would have to use the method of calculus of variations. Obviously, the same piloted simulation data could be used to validate a different approach to the inverse solution problem.

The simple math model used for this study proved to be quite flexible, which aided in setting different levels of MA. This was an important feature for this particular study. In the future it may be desirable to use a high-fidelity helicopter math model, but a more complex model will increase the computational complexity of the inverse solution.

APPENDIX A

MATH MODEL

A six-degree-of-freedom stability derivative model called the enhanced stability derivative (ESD) model was used for this study. The ESD model is basically a nonlinear model with linear aerodynamics. It includes the effect of load factor on the pitch and roll rate damping derivatives, the effect of forward speed on the force derivatives, a collective trim curve, and a ground effect model. The attitude response is rate-type in pitch, roll, and yaw, with automatic turn coordination above 50 knots.

The total aerodynamic forces and moments required for the six-degree-of-freedom equations of motion are generated as the summation of reference and first-order terms of a Taylor series expansion about a reference trajectory. The model includes no control or response coupling. The pitch and roll response is rate command, the yaw response is rate command at low speed with automatic turn coordination above fifty knots. The turn coordination derivatives are ramped in between thirty and fifty knots. A description of each of the individual axes is included below.

Longitudinal Response

The y-axis inertia is eliminated from the moment equation for pitch so that the pitch acceleration is calculated directly:

$$\dot{q} = M_q q + M_{\delta_e} \delta_e \tag{A1}$$

M_q is calculated as a linear function of load factor:

$$M_q = M_{q_m} N_z + M_{q_b} \tag{A2}$$

The value of M_{q_m} was taken from reference 9. A summary of the configuration values that are used for M_{q_m} and M_{q_b} is included in table A1. M_{δ_e} is calculated to provide a constant maximum pitch rate capability independent of the load factor:

$$M_{\delta_e} = M_{\delta_{e_k}} M_q \tag{A3}$$

where

$$M_{\delta_{e_k}} = \frac{-\pi q_{\max}}{180(\delta_{e_{\max}} - \delta_{e_{deadzone}})} \tag{A4}$$

A summary of the values that are used for $q_{\max}$ is included in table 2.

The x-direction acceleration is calculated as follows:

$$\dot{u} = X_u u - g \sin \theta - wq + vr \tag{A5}$$

Table A1. Slope and intercept values used to calculate M_q and L_p

Damping	M_q	M_{q_m}	M_{q_b}	L_p	L_{p_m}	L_{p_b}
low	-1.0	-1.5	0.5	-2.5	-1.5	-1.0
medium	-2.0	-1.5	-0.5	-5.0	-1.5	-3.5
high	-3.8	-1.5	-2.3	-9.5	-1.5	-8.0

37

where

$$X_u = -2.65 * 10^{-4} |u| \tag{A6}$$

Vertical Response

The vertical acceleration is expressed by

$$\dot{w} = Z_w w + Z_{ge} + Z_r + Z_{\delta_c}\delta_c + g\cos\theta\cos\phi - vp + uq \tag{A7}$$

Z_w is considered a function of u and w and determined using a least squares fit of UH-1 stability derivative data taken from reference 10 (see fig. A1).

The ground effect term, Z_{ge}, is calculated by first finding the induced velocity using simple momentum theory:

$$v_i = \sqrt{-\frac{V^2}{2} + \sqrt{\left(\frac{V^2}{2}\right)^2 + \left(\frac{T}{2\rho A}\right)^2}} \tag{A8}$$

where V is the total airspeed in ft/s, ρ is air density (0.002378 slug/ft^3), and A is the disc area (1257 ft^2). Using this value of v_i, thrust IGE over the thrust OGE can be found (ref. 11):

$$\frac{T_g}{T_\infty} = \frac{1}{1 - \frac{1}{16}\left(\frac{R}{z}\right)^2\left[\frac{1}{1+\left(\frac{V}{v_i}\right)^2}\right]} \tag{A9}$$

where R is the rotor radius (20 ft) and z is the disc height above ground. From this expression the ground effect component can be calculated:

$$Z_{ge} = \left(1 - \frac{T_g}{T_\infty}\right)N_z g \tag{A10}$$

Z_r is a reference term required to cancel the effects of gravity and vertical damping in trim:

$$Z_r = -g\cos\theta_{trim}\cos\phi_{trim} - Z_w w_{trim} \tag{A11}$$

where for straight and level flight,

$$\theta_{trim} = \sin^{-1}\left(\frac{X_u u}{g}\right) \tag{A12}$$

$$\phi_{trim} = \sin^{-1}\left(\frac{-Y_v v}{g\cos\theta_{trim}}\right) \tag{A13}$$

$$w_{trim} = \frac{u\tan\theta_{trim}}{\cos\phi_{trim}} - v\tan\phi_{trim} \tag{A14}$$

The reader is reminded that u in this case represents total longitudinal body velocity as opposed to perturbation velocity.

The collective sensitivity term, Z_{δ_c}, is calculated as follows. First, the collective trim position (c_{trim}) is obtained using the trim curve shown in figure A2. Then the minimum and maximum collective inputs are calculated:

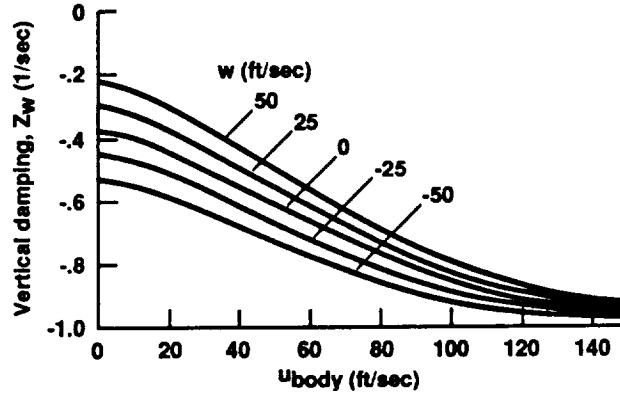$$\delta_{c_{max}} = c_{max} - c_{trim} \tag{A15}$$
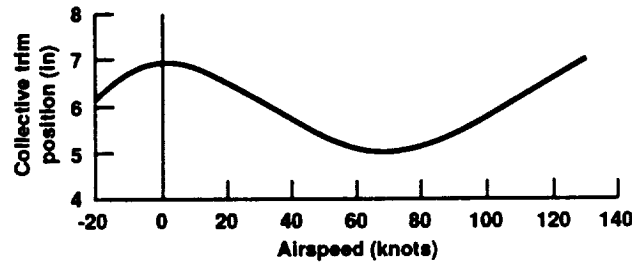
38

Figure A1. Z_w vs. u vs. w.

Figure A2. Collective trim position vs. airspeed (out of ground effect).

$$\delta_{c_{\min}} = c_{\min} - c_{\text{trim}} \tag{A16}$$

The maximum continuous load factor is calculated using a simple expression relating the continuous load factor capability at hover and the load factor capability at the current airspeed:

$$N_{z_{\max c}} = N_{z_{\max c_{\text{hover}}}} \frac{\delta_{c_{\max}}}{\delta_{c_{\max_{\text{hover}}}}} \tag{A17}$$

The three values of $N_{z_{\max c_{\text{hover}}}}$ were 1.34, 2.02, and 2.69 g, which gave a continuous load factor capability at 85 knots ($N_{z_{\max c}}$) of 2, 3, and 4 g, respectively.

Next, the maximum transient load factor is calculated by multiplying the maximum continuous load factor by a constant:

$$N_{z_{\max t}} = (N_{z_{\max c}} - 1) * K_{\text{overshoot}} + N_{z_{\max c}} \tag{A18}$$

The overshoot constants ($K_{\text{overshoot}}$) used are 0.5, 0.375, and 0.333 for the 2-, 3-, and 4-g envelopes, respectively, to keep approximately the same percentage of overshoot capability. The overshoot constant is washed out to zero using a three-second time constant if the load factor is above the continuous limit. When the load factor drops back below the continuous limit, the overshoot factor returns to its original value using the same three-second time constant. The minimum and maximum values of Z_{δ_c} are then calculated:

$$Z_{\delta_{c_{\max}}} = \frac{-gN_{z_{\max t}} + g\cos\theta_{\text{trim}}\cos\phi_{\text{trim}}}{\delta_{c_{\max}}} \tag{A19}$$

39

$$Z_{\delta_{c_{\min}}} = \frac{-gN_{z_{\min t}} + g\cos\theta_{\text{trim}}\cos\phi_{\text{trim}}}{\delta_{c_{\min}}} \tag{A20}$$

The values of $N_{z_{\min t}}$ (above 50 knots) were 0, –0.5, and –1 g for the 2-, 3-, and 4-g envelopes, respectively.

A slope and an intercept are then found as shown here:

$$Z_{\delta_{cm}} = \frac{Z_{\delta_{c_{\max}}} - Z_{\delta_{c_{\min}}}}{c_{\max} - c_{\min}} \tag{A21}$$

$$Z_{\delta_{c_b}} = Z_{\delta_{c_{\min}}} - \delta_{c_{\min}}Z_{\delta_{cm}} \tag{A22}$$

The collective perturbation is the difference between the collective position and the collective trim position:

$$\delta_c = c - c_{\text{trim}} \tag{A23}$$

and this value is used to calculate Z_{δ_c}:

$$Z_{\delta_c} = \delta_c Z_{\delta_{cm}} + Z_{\delta_{c_b}} \tag{A24}$$

Lateral–Directional Response

The roll response of the helicopter is similar to the pitch response, i.e.,

$$\dot{p} = L_p p + L_{\delta_a}\delta_a \tag{A25}$$

L_p is calculated as a linear function of load factor:

$$L_p = L_{p_m}N_z + L_{p_b} \tag{A26}$$

The value of L_{p_m} was taken from reference 9. A summary of the configuration values that are used for L_{p_m} and L_{p_b} is included in table A1. L_{δ_a} is calculated to provide a constant maximum roll rate capability independent of the load factor:

$$L_{\delta_a} = L_{\delta_{a_k}}L_p \tag{A27}$$

where

$$L_{\delta_{a_k}} = \frac{-\pi p_{\max}}{180(\delta_{a_{\max}} - \delta_{a_{\text{deadzone}}})} \tag{A28}$$

A summary of the values that are used for $p_{\max}$ is included in table 2.

The y-direction acceleration is calculated as follows:

$$\dot{v} = Y_v v + g\cos\theta\sin\phi - ur + wp \tag{A29}$$

where $Y_v = -0.08$ 1/sec.

The yaw acceleration is calculated as follows:

$$\dot{r} = N_r r + N_{\delta_p}\delta_p + N_\phi\phi + N_v v + N_p p \tag{A30}$$

where $N_r = -2$ 1/sec and $N_{\delta_p} = 0.6$ rad/sec^2/in. The derivatives N_ϕ, N_v, and N_p are functions of total airspeed and are shown in figures A3, A4, and A5. stability derivatives are scheduled such that weathercock stability exists above 30 knots and automatic turn coordination exists above 50 knots.
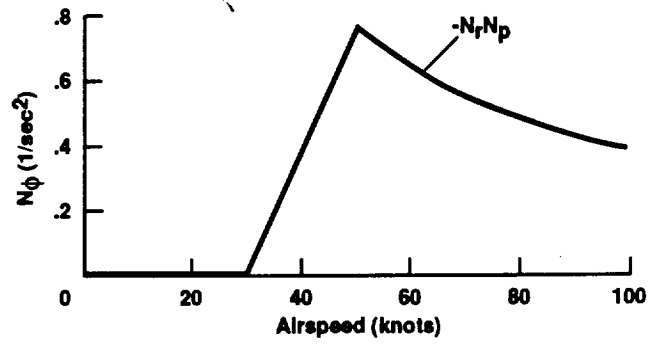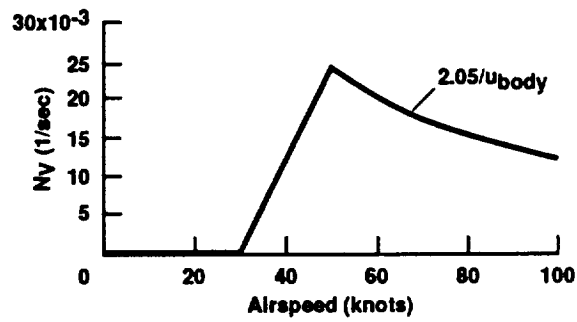
40

Figure A3. N_ϕ vs. airspeed.
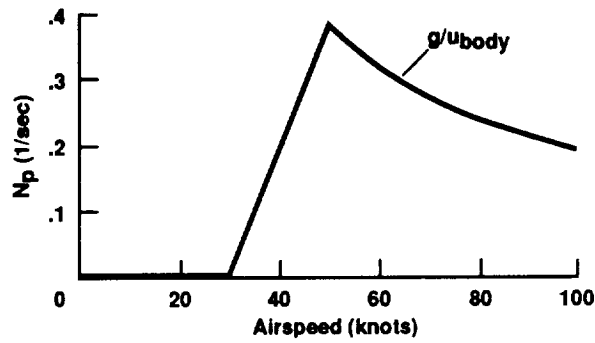
Figure A4. N_v vs. airspeed.

Figure A5. N_p vs. airspeed.

41

APPENDIX B

DEFINITION OF MANEUVERABILITY AND AGILITY

Many authors have tried to define maneuverability and agility (MA) (refs. 12-20). The intent of this appendix is to summarize the definitions that have been given in the past into one definition of MA.

Why Define Maneuverability and Agility?

Before these two critical attributes can be defined, it must first be understood why a definition is needed and in what context it might be used.

In the past, most air vehicle designers have had a general idea of what maneuverability and agility are. Their efforts to increase MA have been focused in areas where the pilot demanded more of what he perceived to be a good thing (load factor or roll rate, for instance). This approach has worked reasonably well in the past, which might lead one to conclude that an attempt to precisely define MA is an unnecessary exercise in semantics. This is definitely not the case.

Technological advances have given today's aircraft designer a myriad of options such as tilt rotors, auxiliary thrusters, high-angle-of-attack control, vectored thrust, etc. This leaves the designer with the difficult task of deciding which of these configuration options will result in the highest mission effectiveness. Even after a configuration is chosen, the relationship between the aircraft design parameters and mission effectiveness is quite complex.

Figure B1 illustrates the relationship between mission effectiveness and MA. Mission effectiveness results largely from the handling qualities of the vehicle. Handling qualities are the combination of flying qualities and other outside factors. To quote from Cooper and Harper (ref. 8):

> The term "Handling Qualities" requires a clear definition in order to emphasize that it includes more than just stability and control characteristics. Other factors that influence the handling qualities are the cockpit interface (e.g., displays, controls), the aircraft environment (e.g., weather conditions, visibility, turbulence) and stress, the effects of which cannot readily be segregated.

Figure B1 diagrams the various interactions between handling qualities and the factors which influence them. Note that it draws a distinction between flying qualities and handling qualities. This set of definitions (proposed by Key, unpublished) provides a convenient structure on which to discuss MA.

As previously stated, the number of permutations required to examine the influence of all design parameters on mission effectiveness is staggering. Suppose, however, that one first determines the flying qualities needed, in terms of maneuverability, agility, stability, and controller characteristics, to achieve the desired mission effectiveness. The designer would then be left with the task of determining which configuration/design best satisfied the desired flying qualities. As a result, the process would be greatly streamlined. Current aeronautical design standards and specifications such as those of reference 13 partially specify the required flying qualities for air vehicles but fail to clearly define and specify MA requirements. A clear definition of MA is required before such a specification can be written.
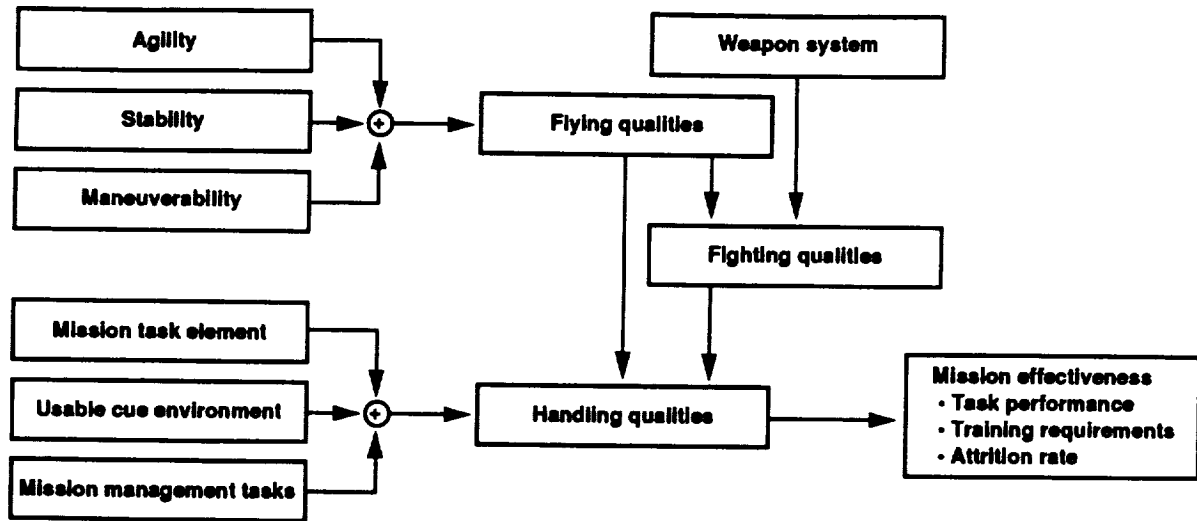
43

Figure B1. Relation of MA to mission effectiveness.

Definitions of Maneuverability and Agility in the Literature

As stated previously, there are many definitions of MA in the literature. The intent of this section is to present and interpret those definitions.

To begin with, Webster's defines maneuverability as the quality or state of being able to make an intended and controlled variation from a straight and level flight path in the operation of an airplane. Agility is defined as the quality or state of being able to move with quick easy grace. These definitions of MA are worth noting because they form a basis on which precise aircraft MA definitions can be constructed. These definitions can be interpreted to mean that maneuverability is the measure of an aircraft's ability to move away from trim, and agility is the measure of an ability to make that move with "quick easy grace." These basic elements are important and will be referred to again in the following paragraphs.

In reference 13, Olson defines maneuverability:

> Maneuverability can be defined as the ability to change the flight path of an aircraft through the application of acceleration. It is primarily a function of the power and thrust margins inherent in the aircraft design. Typical measures are rate of climb and turn rate.

Olson defines agility as follows:

> Agility can be thought of as the rate of change of maneuverability. It is the quickness with which different maneuver states can be entered or exited. Agility depends on control power, damping and handling qualities. The primary measure of agility is the elapsed time to make the desired change in maneuver state. Most maneuvers performed by an aircraft combine the elements of both maneuverability and agility, making it inappropriate to deal with them independently.

44

Olson's definition of maneuverability agrees in general with Webster's definition. It has been generalized, however, to include acceleration ability in all flight phases and not just acceleration away from a straight and level flight condition. This is a useful generalization because we are obviously interested in the ability of the aircraft to return to a steady flight condition from a maneuvering state or to transition from one maneuvering state to another.

Olson's definition of agility as the rate of change of maneuverability is not uncommon. However, it does not contain the element of "quick easy grace" as was stated in Webster's definition. Also, this author would argue that handling qualities depend on agility, not vice versa (see fig. B1). Finally, although it is true that most maneuvers contain both maneuverability and agility, it is this author's contention that they can be defined independently.

In reference 14, Thomson defines agility only, and breaks it into two separate measures: overall agility and inherent agility. He defines overall agility as follows:

> Overall agility is the ease with which a helicopter can change it's position and state with precision, speed, and safety.

Thomson defines inherent agility as

> ...the "configuration" agility of a particular helicopter design. Inherent agility can be quantified analytically while overall agility cannot.

Thomson's definition of agility certainly encompasses the "quick easy grace" aspect. His agility definition also adds the element of safety. Unfortunately, it does nothing to clarify the difference between maneuverability and agility; in fact, it lumps both into the same definition. Also, note the fact that Thomson's definition of inherent agility is encompassed in the box labeled "flying qualities" in figure B1.

Levine defines maneuverability in reference 15:

> Maneuverability can be described as the ability to change the state of the vehicle flight path, either through a change of energy (acceleration along the path) or of direction (application of normal acceleration). It can be measured as the limiting values of load factor, turn rate, climb/descent rate, and accel/decel capability. It is influenced by power margin, rotor aerodynamic limits, and structural constraints.

Levine defines agility:

> Agility can be described as the ability to change the maneuver state. It can be measured in terms of the roll, pitch and yaw time constants, the accuracy or "crispness" of maneuvering, and the pilot workload. Agility is greatly influenced by factors associated with vehicle handling qualities, such as control power, inertia, controls and systems integration, and engine response.

Levine's definition of MA is more thorough than the two preceding definitions; however, this author believes that acceleration along the flightpath and acceleration normal to the flightpath can be

45

grouped together and referred to just as acceleration capability. Also, referring again to figure B1, handling qualities result from MA, stability, and performance, not the other way around.

In reference 16, Houston defines agility only:

> When something is described as agile, the intuitive idea is that it can change speed and position rapidly, even violently, but with absolute precision, in order that its task may be fulfilled in the shortest possible time. This is generally true of aerospace vehicles and so agility embraces two, sometimes separate areas of aircraft design, namely performance and handling qualities.

This definition contains the element of precision but obviously differs from the previously described relationship of MA to flying qualities in its use of the terms performance and handling qualities.

In reference 17, Curtiss defines maneuverability:

> Maneuverability is taken to be associated with the limiting flight paths that are possible for a given rotorcraft.

Curtiss also defines agility:

> Agility is associated with the time required to establish the specific flight path.

Curtiss's definitions are not as precise as some of the previous definitions. However, he does capture the fact that maneuverability is associated with the limiting or maximum capability of the aircraft.

In reference 18, Lappos defines maneuverability as

> ...the measure of the ability to change the velocity vector or energy state.
> Measurables: accelerations, N_x, N_y, N_z; rate of climb
> Predictors: usable specific excess power, P_s; available normal acceleration, N_z
> Typical limitations: engine power output, drivetrain torque, rotating system vibratory loads, stationary system static loads.

He defines agility as

> ...the measure of the time required to change maneuver state.
> Measurables: Control power, handling qualities, pilot ratings, available control margins
> Predictors: Control power/damping relationship, yaw control authority

Lappos's definition of maneuverability is in keeping with the previous definitions. Also of interest (and perhaps more useful to the designer) are the limiting factors which he includes. His definition of agility is not exactly the time-rate-of-change of maneuverability which we have seen previously, but simply a measure of how long it takes to enter and exit a maneuver state. Unfortunately, he fails to define the maneuvering state.

The fixed-wing literature also contains many definitions of MA. Most of the work has been aimed toward defining agility rather than maneuverability. In addition there is a great deal of

46

interest in defining "agility metrics," that is, precise quantitative measures of agility. The following definitions are only a few of the most recent.

In reference 19, Cliff defines agility as

the rate at which one can change the net force acting on the vehicle.

Cliff defines agility here in a way that is common to most of the fixed-wing literature. In this paper he actually defines an "agility vector" which is simply the derivative of the acceleration vector.

In reference 20, several different agility definitions and associated agility metrics are presented. The paper basically summarizes the results of several government and industry conferences on the topic. The following are the agility definitions presented by four of the major participants.

1. General Dynamics:

...the ability to point the aircraft quickly, continue pointing the aircraft, and accelerate quickly. It is a function of maneuverability, as represented by the force equations, and controllability, as represented by the moment equations.

2. Eidetics:

...a higher order function of point performance and maneuverability

Qualitatively, Eidetics separates agility into three components representing (1) acceleration/ deceleration along the flightpath, (2) symmetrical turning perpendicular to the flightpath, and (3) rolling about the velocity vector to reorient the flightpath.

3. Messerschmitt-Boelkow-Blohm (MBB):

Agility is the derivative of the maneuver vector.

They have developed agility metrics by mathematically deriving the "agility vector" from the second derivative of the velocity vector as defined in the Frenet-Serret system. The agility vector is divided into three separate components measuring (1) longitudinal agility, in the direction of the velocity vector; (2) curvature agility, in the direction of the maneuver plane; and (3) torsional agility, representing the rotation of the maneuver plane about the velocity vector. The metric is defined as the peak measured value of the component vs time for a given maneuver.

4. The Air Force Flight Test Center:

Agility is the rate of change of aircraft state with precision and control.

One of the most complete definitions of agility is presented by Mazza in reference 21:

Agility is directly related to the time-rate-of-change of maneuver state (acceleration state). It deals primarily with the *translation* of a moving body in three-space. Also,

47

- Agility is a characteristic exhibited by all bodies in motion.
- "Fundamental" metrics apply equally to all bodies (controlled or uncontrolled).
- Agility sensibly exists in any and all spatial dimensions (1, 2, 3, ...n).
- Agility is a long term property (varying trim states and multiple maneuvers).

Mazza reasons that rotation should be left out of the definition of agility because it is merely a method by which translational agility is generated. For example, an aircraft with a thrust vectoring system is not considered more agile because it can rotate faster, but because the main thrust direction can be altered much more rapidly and therefore the three-space translation characteristics of the aircraft are enhanced. In his paper he develops an agility vector which is expressed in terms of flight test/air-to-air combat relevant terms.

A Final Definition of MA

The following points can be summarized from the preceding maneuverability and agility definitions:

1.   Maneuverability refers to the ability to change both the magnitude and direction of the velocity vector.

2.   Maneuverability is not just related to, or reflective of, the ability to change the velocity vector; it is the measure of the *maximum* rate of change of the velocity vector.

3.   Maneuverability pertains to all regions of the flight envelope.

4.   Agility pertains to the derivative of the acceleration vector.

Also, it is this author's opinion that to include the element of "quick easy grace" in the definition of agility leads to confusion. If one accepts that flying qualities are composed of maneuverability, agility, and stability (as shown in fig. B1), and that stability refers to the response of the aircraft to pilot commands, then one must accept that "quick easy grace" is already implied under the heading of stability. With these points in mind, the following definitions of aircraft MA are offered:

Maneuverability is the measure of the maximum achievable time-rate-of-change of the velocity vector at any point in the flight envelope.

Agility is the measure of the maximum achievable time-rate-of-change of the acceleration vector at any point in the flight envelope.

48

REFERENCES

1. McKillip, Robert M., Jr.; and Perri, Todd A.: Helicopter Flight Control System Design and Evaluation for NOE Operations Using Inversion Techniques. Proceedings of the 45th Annual Forum of the American Helicopter Society, May 1989.

2. Kato, O.; and Suguira, I.: An Interpretation of Airplane General Motion and Control as Inverse Problem. J. Guidance, Control, and Dynamics, vol. 9, no. 2, 1986, pp. 198–204.

3. Kato, O.: Attitude Projection Method for Analyzing Large-Amplitude Maneuvers. J. Guidance, Control, and Dynamics, vol. 13, no. 1, 1990, pp. 22–29.

4. Thomson, D. G.: Development and Verification of an Algorithm for Helicopter Inverse Simulation. Vertica, May 1990.

5. Hess, R. A.; Gao, C.; and Wang, S. H.: A Generalized Technique for Inverse Simulation Applied to Aircraft Flight Control. AIAA Paper 91-0149, January 1990.

6. Thomson, D. G.: Evaluation of Helicopter Agility Through Inverse Solutions of the Equations of Motion. PhD thesis, Univ. of Glasgow, November 1986.

7. Plonsky, John G.: Development of Equations to Improve Deficiencies in the Genhel UH-60A Math Model. NAS2-11058, Sikorsky Aircraft Division, United Technologies Corporation, 1989.

8. Cooper, G. E.; and Harper, R. P.: The Use of Pilot Rating in the Evaluation of Aircraft Handling Qualities. NASA TN-5153, 1969.

9. Chen, R. T. N.: Flight Dynamics of Rotorcraft in Steep High-G Turns. AIAA J. Aircraft, January 1984, pp. 14–22.

10. Heffley, R. K.; Jewell, W. F.; Lehman, J. M.; and Winkle, R. A. V.: A Compilation and Analysis of Helicopter Handling Qualities Data, Vol. One: Data Compilation. NASA CR-3144, 1979.

11. Cheeseman, I. C.; and Bennett, W. E.: The Effect of the Ground on a Helicopter Rotor in Forward Flight. Reports and Memoranda No. 3021, Aeronautical Research Council, September 1955.

12. Olson, John R.; and Scott, Mark W.: Helicopter Design Optimization for Maneuverability and Agility. Proceedings of the 45th Annual Forum of the American Helicopter Society, Boston, May 1989.

13. Anon: Aeronautical Design Standard, Handling Qualities Requirements for Military Rotorcraft. ADS-33C, August 1989.

14. Thomson, D. G.: An Analytical Method of Quantifying Helicopter Agility. Proceedings of the Twelfth European Rotorcraft Forum, Garmisch-Partenkirchen, Federal Republic of Germany, September 1986.

15. Levine, Larry S.; and Warburton, Frank W.: Assessment of Rotorcraft Agility and Maneuverability with a Pilot-in-the-Loop Simulation. Proceedings of the 41st Annual Forum of the American Helicopter Society, May 1985.

16. Houston, S.; and Caldwell, A. E.: A Computer Based Study of Helicopter Agility, Including the Influence of an Active Tailplane. Proceedings of the Tenth European Rotorcraft Forum, August 1984.

17. Curtiss, H. C.; and Price, George: Studies of Rotorcraft Agility and Maneuverability. Proceedings of the Tenth European Rotorcraft Forum, August 1984.

18. Lappos, Nicholas D.: Insights into Helicopter Air Combat Maneuverability. Proceedings of 40th Annual Forum of the American Helicopter Society, May 1984.

19. Cliff, Eugene M.; Lutze, F.; Thompson, B.; and Well, K.: Toward a Theory of Aircraft Agility. AIAA 90-2808-CP, AIAA, August 1990.

20. Bitten, R.: Qualitative and Quantitative Comparison of Government and Industry Agility Metrics. AIAA J. Aircraft, vol. 27, no. 3, 1989, pp. 276–282.

21. Mazza, C. J.: Agility: A Rational Development of Fundamental Metrics and Their Relationship to Flying Qualities. AGARD Flight Mechanics Panel Symposium, October 1990.

REPORT DOCUMENTATION PAGE

Public reporting burden for this collection of information is estimated to average 1 hour per response, including the time for reviewing instructions, searching existing data sources, gathering and maintaining the data needed, and completing and reviewing the collection of information. Send comments regarding this burden estimate or any other aspect of this collection of information, including suggestions for reducing this burden, to Washington Headquarters Services, Directorate for Information Operations and Reports, 1215 Jefferson Davis Highway, Suite 1204, Arlington, VA 22202-4302, and to the Office of Management and Budget, Paperwork Reduction Project (0704-0188), Washington, DC 20503.

1. AGENCY USE ONLY (Leave blank)	2. REPORT DATE	3. REPORT TYPE AND DATES COVERED
	July 1991	Technical Memorandum

4. TITLE AND SUBTITLE

Development and Evaluation of an Inverse Solution Technique for Studying Helicopter Maneuverability and Agility

6. AUTHOR(S)

Matthew S. Whalley

5. FUNDING NUMBERS

505-59-52

7. PERFORMING ORGANIZATION NAME(S) AND ADDRESS(ES)

Ames Research Center, Moffett Field, CA 94035-1000 and Aeroflightdynamics Directorate, U.S. Army Aviation Systems Command, Ames Research Center, Moffett Field, CA 94035-1099

8. PERFORMING ORGANIZATION REPORT NUMBER

A-91020

9. SPONSORING/MONITORING AGENCY NAME(S) AND ADDRESS(ES)

National Aeronautics and Space Administration, Washington, DC 20546-0001 and U.S. Army Aviation Systems Command, St. Louis, MO 63120-1798

10. SPONSORING/MONITORING AGENCY REPORT NUMBER

NASA TM-102889

11. SUPPLEMENTARY NOTES

Point of Contact: Matthew S. Whalley, Ames Research Center, MS 220-7, Moffett Field, CA 94035-1000; (415) 604-3505 or FTS 464-3505

12a. DISTRIBUTION/AVAILABILITY STATEMENT

Unclassified — Unlimited
Subject Category 08

12b. DISTRIBUTION CODE

13. ABSTRACT (Maximum 200 words)

An inverse solution technique for determining the maximum maneuvering performance of a helicopter using smooth, "pilotlike" control inputs is presented. Also described is a piloted simulation experiment performed on the NASA Ames Advanced Cab and Visual System to investigate the accuracy of the solution resulting from this technique. The maneuverability and agility capability of the helicopter math model was varied by varying the pitch and roll damping, the maximum pitch and roll rate, and the maximum load-factor capability. Three maneuvers were investigated: a 180-degree turn, a longitudinal pop-up, and a lateral jink. The inverse solution technique yielded accurate predictions of pilot-in-the-loop maneuvering performance for two of the three maneuvers.

14. SUBJECT TERMS

Helicopter maneuverability, Helicopter agility, Inverse control, Helicopter flying qualities, Helicopter handling qualities

15. NUMBER OF PAGES

56

16. PRICE CODE

A04

17. SECURITY CLASSIFICATION OF REPORT	18. SECURITY CLASSIFICATION OF THIS PAGE	19. SECURITY CLASSIFICATION OF ABSTRACT	20. LIMITATION OF ABSTRACT
Unclassified	Unclassified		